



Research Article

A comparative study on hybrid GA-PSO performance for stand-alone hybrid energy systems optimization

Ayktu Fatih GÜVEN^{1,*}, Nuran YÖRÜKEREN²

¹Department of Electrical and Electronics Engineering, Yalova University, Yalova, 77200, Türkiye

²Department of Electrical Engineering, Kocaeli University, Kocaeli, 41001, Türkiye

ARTICLE INFO

Article history

Received: 20 June 2023

Revised: 31 July 2023

Accepted: 12 September 2023

Keywords:

Cost of Energy; Genetic Algorithm Partical Swarm Optimization; Energy Management System Optimal Sizing Design; Stand-Alone Renewable Microgrid System

ABSTRACT

As global energy demands surge and the environmental implications of fossil fuel dependence become more pronounced, there is an urgent need to transition toward more sustainable and eco-friendly energy alternatives. This underscores the dire need for sustainable, secure, and environmentally friendly energy solutions. To this end, efficient energy management strategies combined with the optimal design of hybrid renewable energy systems are paramount for judiciously harnessing renewable resources. In such systems, wind turbines, photovoltaic panels, diesel generators, and battery storage must be meticulously sized to ensure cost-efficiency, environmental sensitivity, and resilience against unpredictable load variations. Addressing these design challenges, our study emphasized the significance of strategic efficiency, prudential component selection, and system dependability. We designed an off-grid hybrid renewable energy system, incorporating photovoltaic panels, wind turbines, battery storage, and diesel generators, to meet the annual energy requirements of a university campus. After recording data for a full year, which included metrics on solar radiation, wind speed, ambient temperature, and campus load, we developed a model founded on comprehensive energy management strategies. This model aims to identify optimal design parameters, reduce annual costs, achieve sustainable energy benchmarks, and ensure a harmonious power exchange between system components. For optimization, we used an array of algorithms, notably the genetic algorithms, particle swarm optimization, gravity search algorithms, and hybrid algorithms, such as the hybrid genetic algorithm-particle swarm optimization and the hybrid gravity search algorithm-particle swarm optimization, supplemented by the HOMERPro software. Our findings revealed that the integration of photovoltaic panels with battery storage led to an annual system cost of \$671,474.98, a leveled cost of energy of \$0.1800, a total net present cost of \$10,898,221.74, and a renewable energy fraction of 100%. It became evident that the hybrid genetic algorithm combined with particle swarm optimization, when aligned with astute energy management strategies, was more effective in determining optimal design parameters than other methodologies. Through this research, we offer profound insights into the dynamics of hybrid renewable energy systems, serving as a guide for pragmatic design and tangible implementation.

Cite this article as: Güven AF, Yörükere N. A comparative study on hybrid GA-PSO performance for stand-alone hybrid energy systems optimization. Sigma J Eng Nat Sci 2024;42(5):1410–1438.

*Corresponding author.

*E-mail address: afatih.guven@yalova.edu.tr

This paper was recommended for publication in revised form by Editor-in-Chief Ahmet Selim Dalkilic



INTRODUCTION

Background

Due to the escalating levels of global production, electrical energy has emerged as a fundamental element underpinning the development of societies and nations [1]. Thus, power plants often depend on fossil fuels for electricity generation. However, the adverse environmental impacts associated with the increased use of fossil fuels, coupled with the rising energy prices and the growth in global surface temperatures due to heightened emission rates, have become untenable [2]. It is reported that a significant portion of the world's fossil fuel originates from coal, primarily used for electricity generation. This has led to increased greenhouse gas emissions, contributing to global warming and obstructing sustainable lifestyles [3]. Turkey's new climate policy underscores the importance of reducing greenhouse gas emissions, particularly given their significant role in climate change during energy production. A strategic plan is required to phase out fossil fuels, eliminate fossil fuel support and incentives, allocate public resources to renewable energy investments, particularly solar and wind energy, build the necessary infrastructure, and establish equitable transformation plans encompassing all sectors [4]. Furthermore, the new climate policy should prohibit the construction of new coal plants, positioning Turkey as a frontrunner in the shift away from coal. The transition away from fossil fuels, alongside other measures aimed at combating climate change, holds promise for improved air quality and technological growth in social life. As a result, developing countries such as Turkey are investing considerable efforts to upgrade their energy infrastructure and curtail environmental pollution, especially greenhouse gas emissions. It is clear that reducing fossil fuel consumption, curbing global warming, and achieving future decarbonization hinge on the utilization of renewable energy for green energy production [5]. Moreover, environmentally friendly and sustainable renewable energy sources (RES) should be tapped into to lessen dependence on other countries and reduce energy costs [6]. The deployment of hybrid renewable energy systems (HRES), which combine renewable energy technologies with energy storage devices, is critical to meeting load demands in remote areas lacking grid access and fostering wider adoption of sustainable energy technologies [7]. In addition, the stochastic characteristics of various RESs and their inherent uncertainties must be offset by each other. However, a storage and backup system is essential to manage the ongoing load demand. Storage options can serve as a buffer to redress the imbalance between supply and demand, thereby augmenting the reliability of HRES. The optimal sizing of the HRES configuration, following RES and load level considerations, is among the most critical decisions taken during the planning phase. The goal is to fulfill the load demand at the chosen location at the lowest possible cost. Therefore, an efficient methodology and model for optimization are indispensable [8].

Literature Review

A variety of configurations and applications are favored by researchers when designing the most efficient HRES. Cao and colleagues demonstrated that, for six major Iranian cities relying on solar-wind energy systems in diverse climates and off-grid homes, wind turbines (WT) and photovoltaic panels (PV) can generate power more consistently throughout the year, despite having similar rated power [9]. Zeljkovic et al. [10] employed Monte Carlo simulations to design an independent HRES for an intercom base station. Using the DIRECT optimization method, they managed to decrease the overall system costs and achieve stable convergence. Mahmoudi et al. employed a fuzzy logic controller and gravity search algorithms to obtain an optimal HRES. In their study, they examined two scenarios: one with a battery coupled with PV and WT, and another that employed a diesel generator (DG) during power outages. Their reliability analysis suggested that replacing the battery storage with a DG made PV/WT/DG the most cost-effective option [11]. Ma et al. researched a standalone renewable energy system for 200 homes on Persian Gulf islands. They applied two optimization methods: load following (LF)-controlled and cycle charging (CC) mode. The LF-controlled mode showed a slightly better cost profile than the CC mode [12]. In China, Xu and colleagues developed an off-grid microgrid system utilizing solar and battery energy for affordable green electricity in rural buildings. Through a year's worth of real data, they derived an optimal size and proposed the taboo search algorithm for ideal sizing. Their experiments suggested reduced costs and fewer batteries and PV in a basic scenario [13]. Yi et al. highlighted the influence of battery storage (BS) types on sizing autonomous PV/BS systems [14]. Aziz et al. combined HOMERPro and MATLAB to optimize an HRES comprising batteries, diesel, and wind. They noted that slight changes in distribution strategies have a pronounced effect on system efficacy [15]. Dufo-López et al. introduced a wind-PV/BS/DG HRES with a thermoelectric generator. Using a genetic algorithm, they identified an economically viable design [16]. Yu et al. suggested a two-stage stochastic optimization approach for HRES design and operation [17]. Some researchers have delved into the combined optimization of system design and demand-side management, viewing it as a form of virtual energy storage [18]. Fares et al. compared ten metaheuristic optimization methods for a standalone HRES. They found the firefly optimization algorithm to be the fastest, whereas simulated annealing was the most accurate and robust [19]. Jasim et al. optimized EMS sizing for an off-grid hybrid microgrid system. They confirmed the superiority of the hybrid gray wolf optimization cuckoo search (GWOCS) algorithm over others like particle swarm optimization (PSO), genetic algorithm (GA), GWO, and CS [20]. Afolabi and colleagues tailored their study to rural Nigerian settlements, proposing an optimal off-grid HRES. They devised a model using a metaheuristic PSO technique, complemented by a fuzzy logic-controlled EMS [21].

Rangel et al. aimed to curtail fuel consumption, costs, and emissions in DG/PV/BS HRES for rural electrification. Their model considered the fuel consumption for diesel-hint oil blends and two primary pollutants. Sensitivity analysis revealed that varying fuel costs had minimal levelized cost of energy (LCOE) impact unless diesel prices surged by 100% [22]. Leandro et al. addressed multi-objective optimization for hybrid wind-PV generation and battery storage. They employed the normal boundary intersection for multi-objective optimization, examining indicators such as net present value, return on investment, and greenhouse gas emissions [23]. Hariri et al. experimentally examined the impact of forced convective cooling on the performance of photovoltaic thermal (PV/T) collectors modified with paraffin and steel foam. The results obtained with two different finned heat sink attachments indicate that this cooling technique can significantly enhance the electrical and thermal efficiency of PV/T collectors [24]. In the work of Khalili and Sheikholeslami, the lack of effective cooling in PV cells was addressed using a numerical approach. They increased the electrical output by adding a thermoelectric layer beneath the Tedlar layer. For cooling the cells, they employed cooling channels of various shapes (circular, triangular, and 3-lobed) using a hybrid nanofluid. The highest performance was achieved with the finned triangular duct, which exhibited a performance 9.97% superior to the circular duct [25]. Jasim and colleagues aimed to integrate demand-side management into residential energy, facilitating informed energy consumption decisions and enabling energy companies to manage peak demand. They employed algorithms such as the binary orientation search algorithm (BOSA), cockroach swarm optimization, and the sparrow search algorithm. Notably, BOSA stood out with its lower standard deviation and cost savings compared to other algorithms [26]. Akdamar et al. demonstrated how the efficiency of solar air heaters could be enhanced by harnessing the waste heat produced from cooling photovoltaic modules. In their experiment, two distinct solar air heaters were used: the first (hybrid) was equipped with a heat exchanger, and the second operated as a standard unit. Remarkably, the hybrid unit yielded an air temperature 18.13% higher than the standard unit. This innovative approach enabled the recovery of 188.64 kWh of waste heat annually in the hybrid unit, resulting in an annual CO₂ emissions reduction of 144 kg [27]. Amuta et al. assessed an isolated solar/battery microgrid, focusing on optimizing energy resource integration for a remote Nigerian community. Using the annualized system cost, a 25-year cost of energy (COE) was examined. Using MATLAB-based Particle Swarm Optimization, the optimal configuration was established. Their findings suggest that the proposed microgrid model offers valuable insights for economic microgrid design, confirming its viability in various global scenarios [28]. In a study by El-Khozondar and colleagues, the focus was on addressing the electricity crisis in Gaza, which was exacerbated by political tensions and the

COVID-19 pandemic. To this end, a off-grid HRES was proposed as a viable solution for powering quarantine centers. Utilizing the HOMER-Pro program for simulation and optimization, it was determined that a combination of PV, wind, and diesel generators in the HRES configuration presented the most cost-effective solution compared to traditional systems. The recommended HRES comprised of a 150 kW PV, a 200 kW wind turbine, and two diesel generators of capacities 500 kW and 250 kW, respectively. Impressively, the system promises a payback period as short as 1.8 years. The findings of this research offer a practical and sustainable approach for powering critical facilities such as quarantine centers [29]. In a study conducted by Kely and colleagues, it was highlighted that Chad's energy production relies entirely on thermal plants utilizing fossil fuels, which are not environmentally friendly. Moreover, the electrification rate in Chad is less than 11%. The research aimed to propose reliable electrification alternatives for Chad through hybrid energy systems. To realize this objective, the feasibility of autonomous hybrid PV/WT/DG/BS systems to meet the electrical demand in Chad's isolated regions was evaluated using the HOMER software. Three types of daily load profiles in each of the 16 unelectrified regions in Chad were considered: low, medium, and high community load profiles. The simulations revealed optimal configurations of PV/BS, PV/DG/BS, and PV/WT/DG/BS for various consumers and sites. The COE ranged from 0.367 to 0.529 US\$/kWh. This suggests that the COE for some sites is below Chad's production cost of 0.400 US\$/kWh, rendering them economically viable. Implementing these hybrid systems, in comparison to a single diesel generator, would lead to a reduction in CO₂ emissions per year, ranging from 0 to 15,670 kg/year [30]. Therefore, advanced optimization methods must be employed in clean microgrid systems to generate low-cost and sustainable green electricity.

Research Gap

The literature review highlights optimization techniques for power management and sizing of HRES. Researchers use specific software tools for performance analysis during this optimization. These tools fall into two main categories: traditional and metaheuristic optimization techniques. However, such software often demands more computational time compared to traditional methods [31]. Many scholars recommend both traditional and evolutionary algorithms for identifying the optimal HRES component size. Evolutionary algorithms have effectively addressed issues of becoming trapped in local minimums during optimization. Regardless of the approach used, determining the optimal size for HRES always necessitates the use of optimization techniques [32].

This study's distribution strategies prioritize the use of RES over diesel generators to meet load demand. In line with the energy management system's guidelines, batteries were charged without resorting to diesel generators first. Using

the optimization techniques we developed, we assessed the HRES operating conditions. The model's input parameters guided the optimization of the best PV-WT system. Our preliminary simulations employed HOMERPro software, which is the global standard for microgrid design optimization. This software validated our study's sizing method. The simulation results indicate that the leveled unit energy cost from HOMERPro outperforms four different meta-heuristic algorithms. A key distinction between our method and the HOMERPro model is the distribution strategy: the latter allows a diesel generator unit to charge the battery bank without always prioritizing RES. This difference underscores the need for meticulous strategy selection, given the profound influence of HRES on both economic and reliability assessments. Our analysis of the meta-heuristic algorithms used in this study highlights the benefits of hybrid algorithms. They strike a balance between discovery and application. Every optimization algorithm can predict tendencies toward optimal solutions. Notably, the Genetic Algorithm Particle Swarm Optimization (GAPSO) excels in speed when pitted against other popular algorithms and the HOMERPro software.

Paper Organization

The article is structured into several sections. Section II introduces a mathematical model of the HRES components. Section III delves into the objective function, the method, deployment strategies for energy management systems, and metaheuristic algorithms. Optimization outcomes, discussions, and sensitivity analyses are detailed in Section IV. Section V concludes the article.

MATERIALS AND METHODS

This section delves into the measurement data. It also covers the mathematical expressions of energy source power and the formulae for economic analysis. Specific constraints and an objective function were established to address the optimization challenge. The optimization process is comprehensively described at the end. The process graph for the research methodology is illustrated in Figure 1. Each HRES component slated for installation is documented. Their techno-economic parameters, meteorological data, and load demand data are archived in a database. We employed metaheuristic optimization algorithms in the MATLAB environment. Using these algorithms, the optimal size of the HRES is determined. This is done by taking into account the objective function and constraints. The sizing process yields detailed insights. It provides the system's energy profile for each second over a year. This profile is based on comprehensive energy data and graphs.

Hybrid Renewable Energy System Modeling

This study examines six essential components of the HRES. Three of these components are related to DC electricity: the PV plant, battery pack, and dump load. The other three, the domestic load, diesel generator, and wind farm, are associated with AC electricity. IGBT-based high-power converters handle both AC to DC and DC to AC conversions. However, the optimization formulation does not account for the dynamics of the transducers because of their relation to high frequencies. An energy management

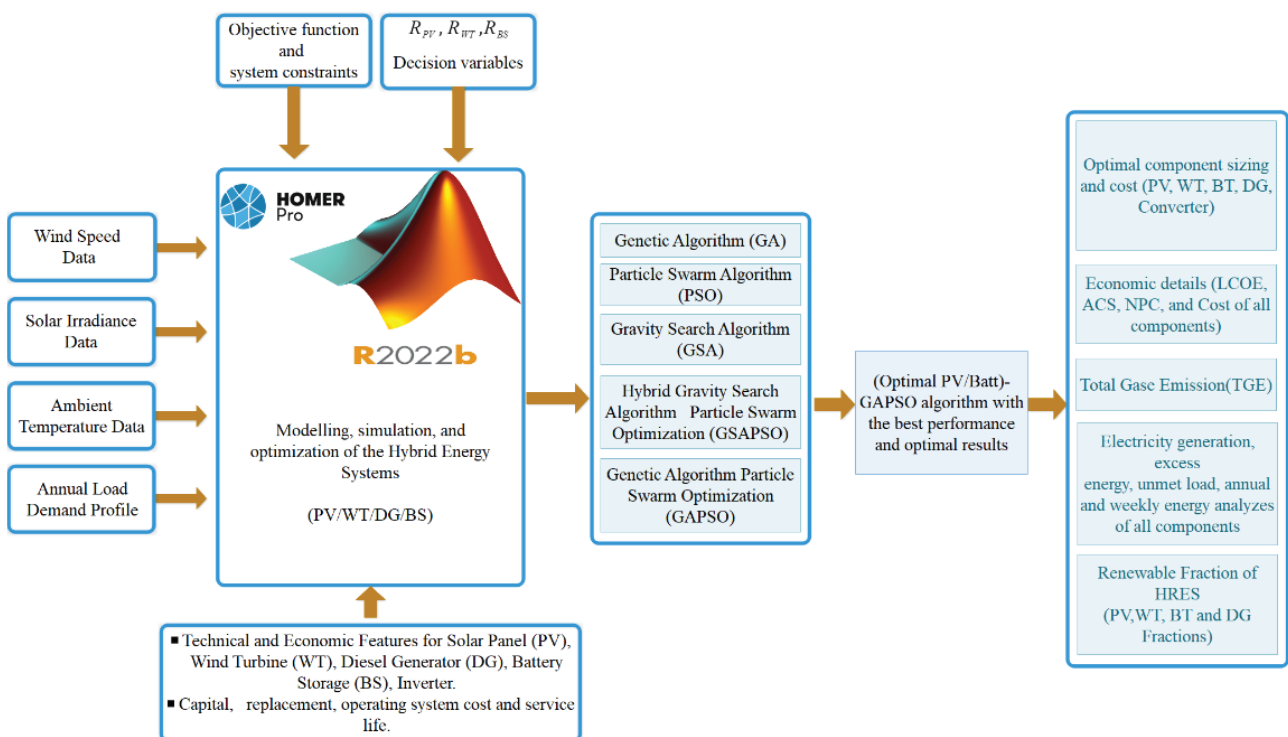


Figure 1. Block diagram of the research methodology.

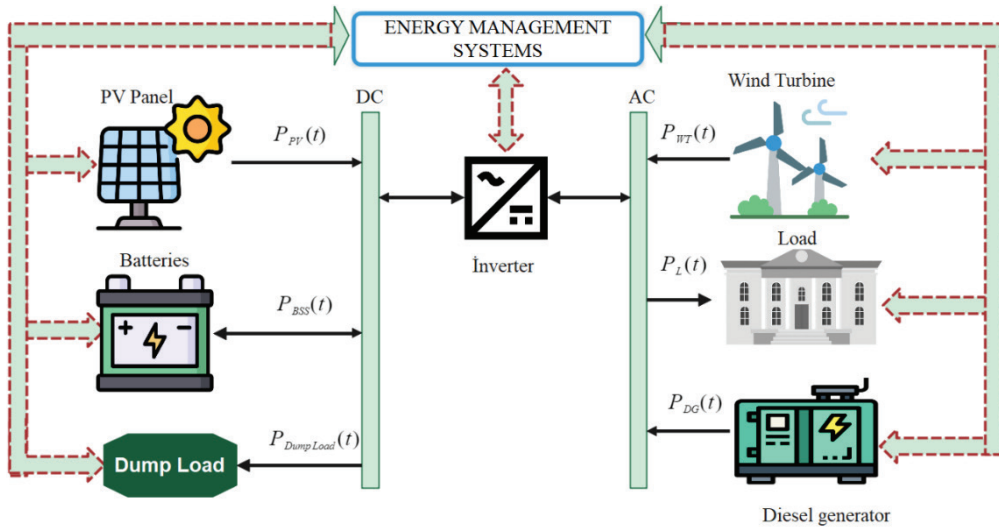


Figure 2. Schematic drawing of the off-grid PV/WT/DG/BS components.

system (EMS) oversees the power distribution among the HRES components. As illustrated in Figure 2, the microgrid configuration features a single DC/AC inverter for power conversion, and the HRES is structured with distinct AC and DC busses. All production elements, loads, and DC/AC converters maintain bi-directional communication with the EMS, continuously updating it with their component statuses. For optimal HRES functioning, the EMS dispatches control signals to each device. Before finalizing the optimal microgrid size, it is essential to model the system components. Because the characteristics of the hybrid system components significantly influence the system's cost of energy (COE) and reliability, a detailed model of these parts is provided in the subsequent section [33].

Photovoltaic Energy System Modeling

The combined power generated by the solar panels in a PV system equals the total power produced by the system. Equation (1), often referred to as the simplified PV model, uses ambient temperature and solar radiation to calculate the power produced by each panel per hour [34].

$$P_{pvout}(t) = P_{(PVrated)} \times \frac{G}{1000} [1 + \alpha_c (T_{amb} + (0.0256 \times G)) - T_{ref}] \quad (1)$$

Here, $P_{pvout}(t)$ the PV module's output power (W), G solar radiation value (W/m^2), and $P_{(PVrated)}$ PV nominal power value (W) in standard test conditions. The temperature coefficient defined by $\alpha_c (-3.7 \times 10^{-3} (1/^\circ C))$, T_{ref} denotes the standard test conditions temperature of the PV cell ($^\circ C$), and T_{amb} ambient temperature ($^\circ C$).

Modeling of Wind Energy System

The most accurate model is essential for estimating the power output from a WT. The determining factor for a wind turbine's power output in any given locale is the wind speed. The power produced by the wind turbine is computed using Equation (2).

$$P_{WT} = \begin{cases} 0 & v(t) \leq v_{cut-in} \text{ or } v(t) \geq v_{cut-out} \\ P_r \times \frac{v(t) - v_{cut-in}}{v_r - v_{cut-in}} & v_{cut-in} \leq v(t) \leq v_r \\ P_r & v_r \leq v(t) \leq v_{cut-out} \end{cases} \quad (2)$$

P_r represents the WT nominal power (kW), $v(t)$ represents the wind speed (m/s), $v_{cut-out}$ represents the low shear speed of WT (m/s), v_r represents the WT nominal speed (m/s), and v_{cut-in} represents the high shear speed values of WT (m/s).

$$v(t) = v_{ref}(t) \times \left(\frac{H}{H_{ref}}\right)^{a_h} \quad (3)$$

In Equation (3), establishes a relationship between the wind speed at the reference hub height ($v(t)$) and the wind speed at the anemometer height (v_{ref}), along with the heights of the anemometer (H_{ref}) and wind turbine hub (H), as well as the exponential power law values (a_h).

The coefficient a_h is influenced by surface roughness and environmental stability, typically ranging from 0.05 to 0.5. For the selected sites in this study, a_h is taken as 0.14 [35].

Battery Storage System Modeling

A storage system is necessary to regulate fluctuations in renewable energy generation and ensure that it aligns with the load demand. When the energy generated by RES surpasses the total load demand, the batteries are charged. On the other hand, if the power generated falls short of the load demand, the batteries are depleted to compensate for the energy gap. The processes of battery discharging and charging are assessed using Equations (4) and (5), respectively [36].

$$E_{ch}(t) = E_{BS}(t-1) \times (1 - \sigma) + \left[E_{WT}(t) + E_{PV}(t) - \frac{E_L(t)}{\eta_{inv}} \right] \times \eta_{BC} \quad (4)$$

$$E_{dch}(t) = E_{BS}(t-1) \times (1 - \sigma) + \left[\frac{E_L(t)}{\eta_{inv}} - (E_{WT}(t) + E_{PV}(t)) \right] \times \eta_{BD} \quad (5)$$

In the described equation, several components related to the battery storage system (BSS) and energy production

play pivotal roles. The capacity of the BS at a specific time t is signified by $E_{BS}(t)$ in kWh, while its capacity from the preceding hour, $(t-1)$, is expressed as $E_{BS}(t-1)$. During the hour t , the energy demand is captured by $E_L(t)$. Concurrently, E_{WT} quantifies the energy produced by the wind turbine. The BSS's self-discharge rate, a critical factor, is denoted by σ and lies between 0 and 1. Additionally, the PV panel's contribution to energy at time t is indicated by E_{PV} . The efficiencies associated with charging and discharging the BSS are represented respectively by η_{BC} and η_{BD} . While these efficiencies can fluctuate based on the current at distinct charging stages, this study assumes a consistent 90% charging efficiency. Lastly, the inverter's operational efficiency in the system is encapsulated by η_{inv} .

In order to limit battery capacity, excess power generated RES is stored in BS. However, it is important to note that BSs have a limited capacity for storing energy. If a BS is fully charged and cannot store any more excess power from RES, that excess power must either be discharged or wasted. Overcharging the BS can damage the batteries and shorten their lifespan. Therefore, it is crucial to discharge excess power in a controlled manner to prevent this issue. A critical parameter to consider in this context is the maximum allowable depth of discharge (DOD), expressed as a percentage. For this study, the DOD was assumed to be 80%. The minimum BS capacity was determined using Equation (6) [37].

$$v(t) = v_{ref}(t) \times \left(\frac{H}{H_{ref}}\right)^{a_h} \tag{6}$$

In addition, the BS capacity restriction at any hour was expressed by Equation (7).

$$E_{BSmin} \leq E_{BS}(t) \leq E_{BSmax} \tag{7}$$

Here, the DOD maximum permissible depth of BS discharge (%), E_{BSmax} and E_{BSmin} are the BS's maximum and minimum capacities, respectively.

Modeling of Diesel Generator

While generators are not viewed as a renewable energy source due to their substantial operational emissions, they can be reliable in circumstances where RES are insufficient or energy storage is exhausted. Diesel generators' fuel consumption and efficiency are crucial in HRES design, as depicted in Equation (8) [38].

$$q(t) = a_{dg} \times P_{DG}(t) + b_{dg} \times P_r \tag{8}$$

In the equation, $P_{DG}(t)$ represents the power output of DG at hour t (kW), $q(t)$ represents consumption of fuel (L/h), P_r represents average DG power, while a_{dg} and b_{dg} (L/kW) are constants that represent the parameters of standard fuel consumption, which were 0.246 and 0.08415, respectively.

Modeling of Inverter

An inverter is a piece of electronic equipment that converts the DC power generated by RES into AC. Equation (9) can be used to calculate the inverter's input power (P_{inv}) [39].

$$P_{inv}(t) = P_L(t) / \eta_{inv} \tag{9}$$

Here, $P_L(t)$ and η_{inv} are load power and inverter efficiency respectively.

Data on the Economic Parameters of the Energy System

For a comprehensive financial analysis, it is essential to consider the impact of sensitive variables influencing the

Table 1. Economic and technical Specifications of Microgrid Components

Definition	Parameters	Values	Units
A. PV	Rated capacity	0.345	kW
	Temperature coefficient	-0.390	
	Operating temperature	44	°C
	Efficiency	17.8	%
	Lifespan	20	Years
	Capital cost	650	\$/kW
	Replacement cost	650	\$/kW
	Maintenance and Operation cost	50	\$/year
B. WT	Rated power	1	kW
	Hub height	17	m
	Installation cost	2000	\$/kW
	Replacement cost	2000	\$/kW
	Maintenance and Operation cost	200	\$/year
	lifespan	20	Years
C. BSS	Rated voltage	600	V
	Rated capacity	100	kWh
	Capacity(max)	167	Ah
	Round-trip efficiency	90	%
	Charging current (max)	167	A
	Charge status (min)	20	%
	Discharge current (max)	500	A
	Dept of discharge	80	%
	Lifespan	10	Years
	Capital cost	550.00	\$/kW
Replacement cost	550.00	\$/kW	
D. DG	Capacity	1500	kW
	Replacement cost	250	\$/kW
	Maintenance and Operation cost	30	\$/kWh
	Capital cost	175	\$/kW
	Fuel price	1	\$/L
	Lifespan	10	Years
E. Inverter	Capacity	1	kW
	Maintenance and Operation cost	50	\$/year
	Capital cost	300	\$/kW
	Replacement cost	300	\$/kW
	Efficiency	95	%
Lifespan	15	Years	
F. Economic Parameters	Interest rate	20	%
	Inflation rate	17	%
	Discount rate	9	%
	lifespan	20	Years

feasibility of the HRES. The economic parameters adopted in this study include a 19% real interest rate, a 17% inflation rate, and a 9% discount rate, with the HRES having an anticipated lifespan of 20 years. Manufacturers provided the actual costs or pricing details of the HRES components used in the simulations. Table 1 presents both the technical and economic specifications of the components that make up the HRES.

Analysis of Campus Energy Consumption

The investigation targeted a university campus, with Figure 3 showcasing the spatial coordinates of the study area. Meteorological data for 2022 were sourced from the State Meteorology General Directorate specific to the research site. These data include hourly wind speed, solar radiation, ambient temperature, and annual load curves. The university's peak hourly load reached approximately 1,281.23 kW, with the lowest demand recorded at 425.84 kW. The average daily electricity consumption amounted

to 10,220.26 kWh. Figure 4 illustrates the load profile spanning a year, encompassing 8,760 hours, for the chosen case study. This profile was derived from actual data collected from the research area.

Meteorological Data

For accurate sizing of an HRES, we harnessed the capabilities of both HOMERPro and MATLAB platforms. MATLAB is particularly recognized for its proficiency in multi-objective optimization related to HRES. This software can deploy numerous algorithms to identify optimal system configurations tailored to specific geographic areas. Before initiating computational processes in MATLAB, the consumption patterns or load profile of the designated area must be considered. Moreover, MATLAB requires a comprehensive set of data on the technical and economic specifications of the system elements, alongside hourly meteorological data. These data should cover aspects such



Figure 3. Location of the case study (Turkey).

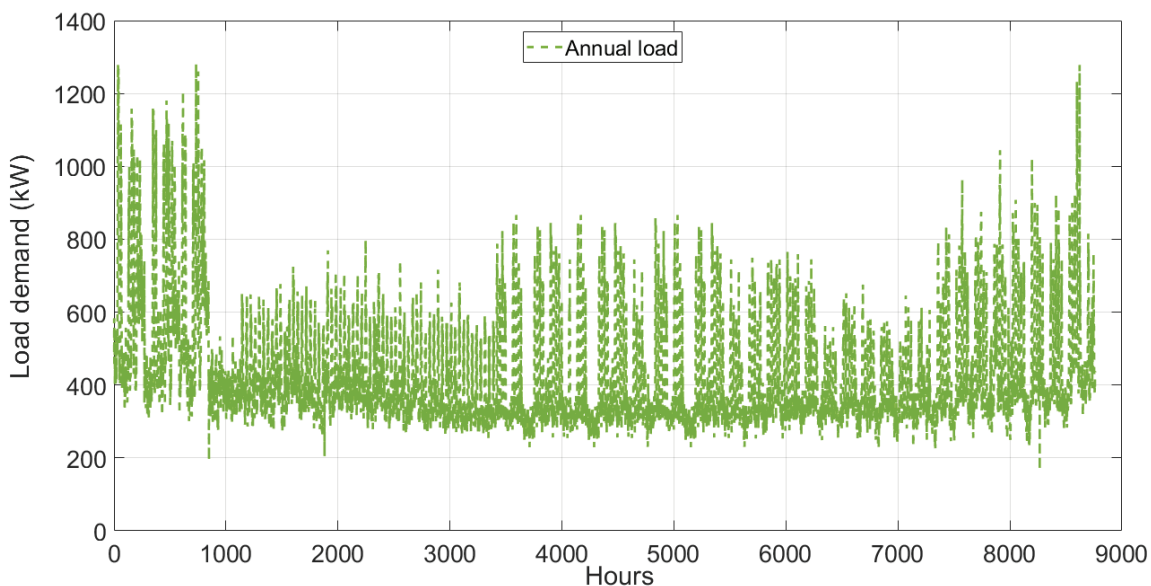
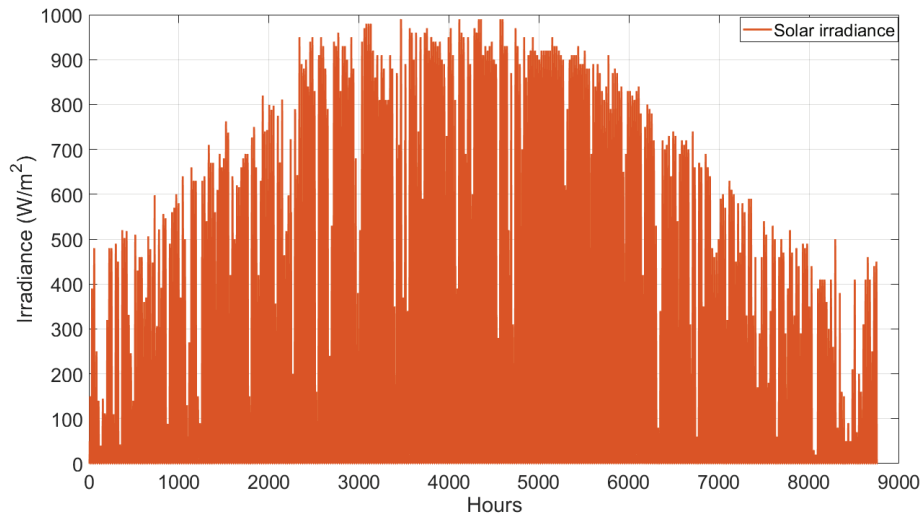
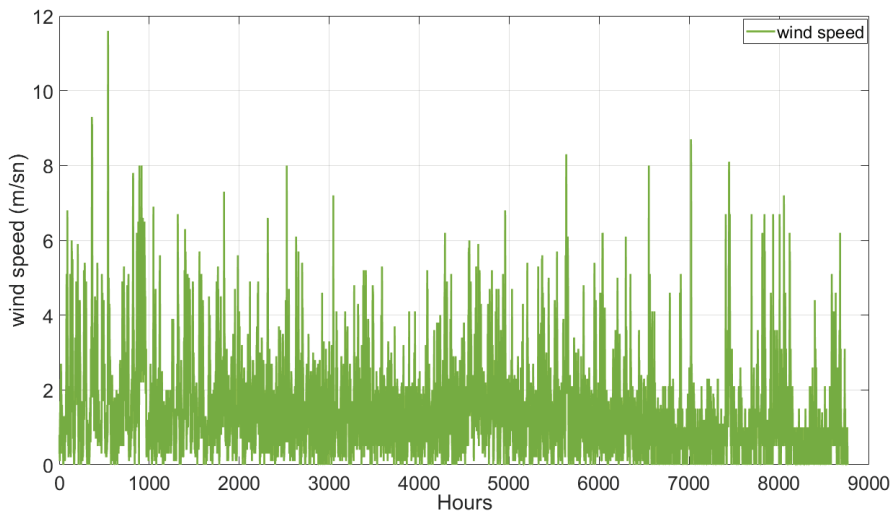


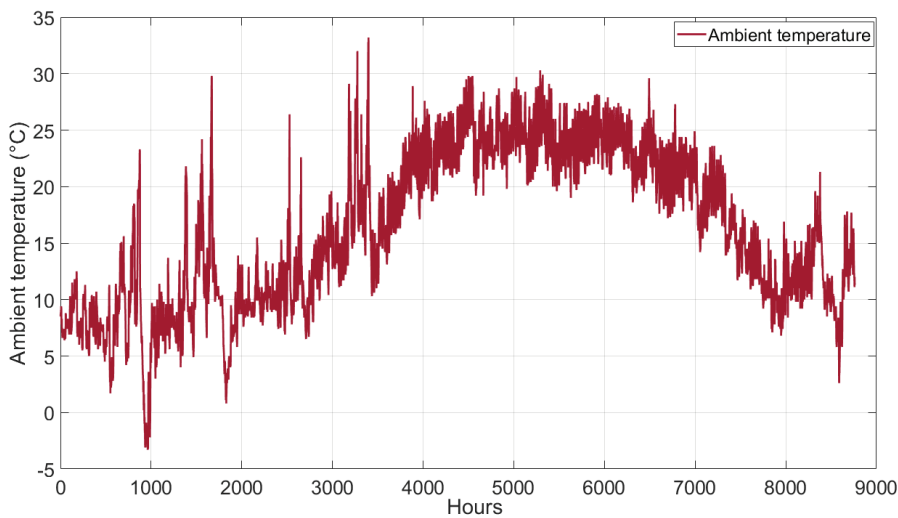
Figure 4. Yearly electricity demand curve of the campus.



(a)



(b)



(c)

Figure 5. Weather patterns of the study area. (a) solar radiation (W/m^2), (b) wind speed (m/s), and (c) ambient temperature ($^{\circ}C$).

as solar irradiance, surrounding temperature, and wind velocities. The annual hourly distributions of wind velocity, solar irradiance, and surrounding temperatures are depicted in Figures 5(a), 5(b), and 5(c) in sequence.

METHODOLOGY

HRES combine various renewable sources to ensure stable power production. However, their design is influenced by meteorological data because the power profiles of renewables can differ greatly. The optimization of HRES should account for both power generation demands and renewable energy outputs. This demands precise component sizing that is reliant on meteorological parameters. Proper sizing and selection of the right components are essential. They are pivotal in enhancing efficiency and system stability, paving the way for a shift toward sustainable energy. The subsequent chapter delves into the methodology used in this study. This section covers the HRES sizing process, energy management strategy, objective function, and optimization algorithms.

Energy Management System (EMS)

The energy management strategy is designed to effectively manage the power produced by RES, with the key goal of minimizing energy waste. In this study, we focus on optimizing HRES usage. This involves regulating the power produced by the RES and overseeing the charge and discharge cycles of the battery storage system. In addition, a diesel generator acts as a backup power source, supplementing the campus's energy needs when the RES falls short of demand [40]. Depending on the loop charging strategy, the EMS controller operates under various scenarios.

Case 1: Wind and solar energy sources provide enough energy to meet the load demand, and excess energy from these sources will charge the BS ($E_{BS}(t) < E_{BSmax}(t)$).

Case 2: The surplus energy generated by wind and solar sources is effectively harnessed and used to its fullest potential by storing it for future use or by employing it in alternative ways rather than letting it go to waste ($E_{BS}(t) = E_{BSmax}(t)$).

Case 3: if the energy produced by the wind and solar sources falls short of the required load demand, the energy stored in the battery banks will be utilized to ensure that the demand is met ($E_{BS}(t) > E_{BSmin}(t)$).

Case 4: In situations where the wind and solar sources fail to generate enough energy to meet the load demand and the battery banks are depleted, the diesel generator is activated to provide the needed energy and simultaneously recharge the batteries. As soon as the RES resumes generating power, the diesel generator ceases operation automatically ($E_{BS}(t) < E_{BSmin}(t)$).

Figure 6 illustrates the power-flow algorithm strategy for the EMS intended for the university campus. This algorithm operates continuously to optimize energy consumption and minimize wastage. To guarantee a consistent

power supply in an HRES, a management strategy that draws upon backup energy sources, such as battery banks and a diesel generator, is implemented. The strategy begins by collecting input data, including load demand, climatic conditions, wind power, and solar power. The management procedure then evaluates the total energy produced by renewable sources against the energy demand, activating backup sources when required.

Hybrid energy system objective function

The central objective in analyzing the HRES is to determine the average system cost. The goal is to configure the system to supply dependable power at the most economical rate. The ideal setup is established by considering three primary decision factors: the number of batteries, WT power, and PV power. The lowest annual cost of the system (ACS) emerges as the optimal outcome, considering all other parameters and constraints in the techno-economic analysis [41]. The objective function encompasses the total initial and replacement expenditures, in addition to the operation and maintenance costs. Costs tied to installation and construction are incorporated within the capital costs of the components. Relevant decision factors include ACS, LCOE, TNPC, PV, WT, DG, BS, and inverter capacities.

Total Net Present Cost (TNPC)

The total net present cost (TNPC) quantifies the overall cost associated with the components of an energy system. This cost considers both the expenses and profits generated throughout the system's lifespan. Specifically, it covers the capital, replacement, and operation and maintenance costs for each component. Equation 10 provides the mathematical representation of the TNPC [42].

$$TNPC = \frac{C_{ann_total}}{CRF(i,n)} \quad (10)$$

Here, C_{ann_total} represents the total annual cost in (\$), i represents the actual discount rate as a percentage (%), and n represents the lifespan of the project in years.

One way to represent the capital recovery factor (CRF) is as follows:

$$CRF(i_r, n) = [i_r \times (1 + i_r)^n] / [(1 + i_r)^n - 1] \quad (11)$$

The real discount rate, i , can be expressed as follows:

$$i_r = \frac{i' - r}{1 + r} \quad (12)$$

Here, i' is the nominal interest rate and r is the annual inflation rate. In this study, a discount rate of 9 % and an inflation rate of 17% are assumed.

Levelized cost of energy (LCOE)

The LCOE is a metric used to measure the cost of energy per unit from a specific source, allowing for the comparison of economic performance across various energy sources.

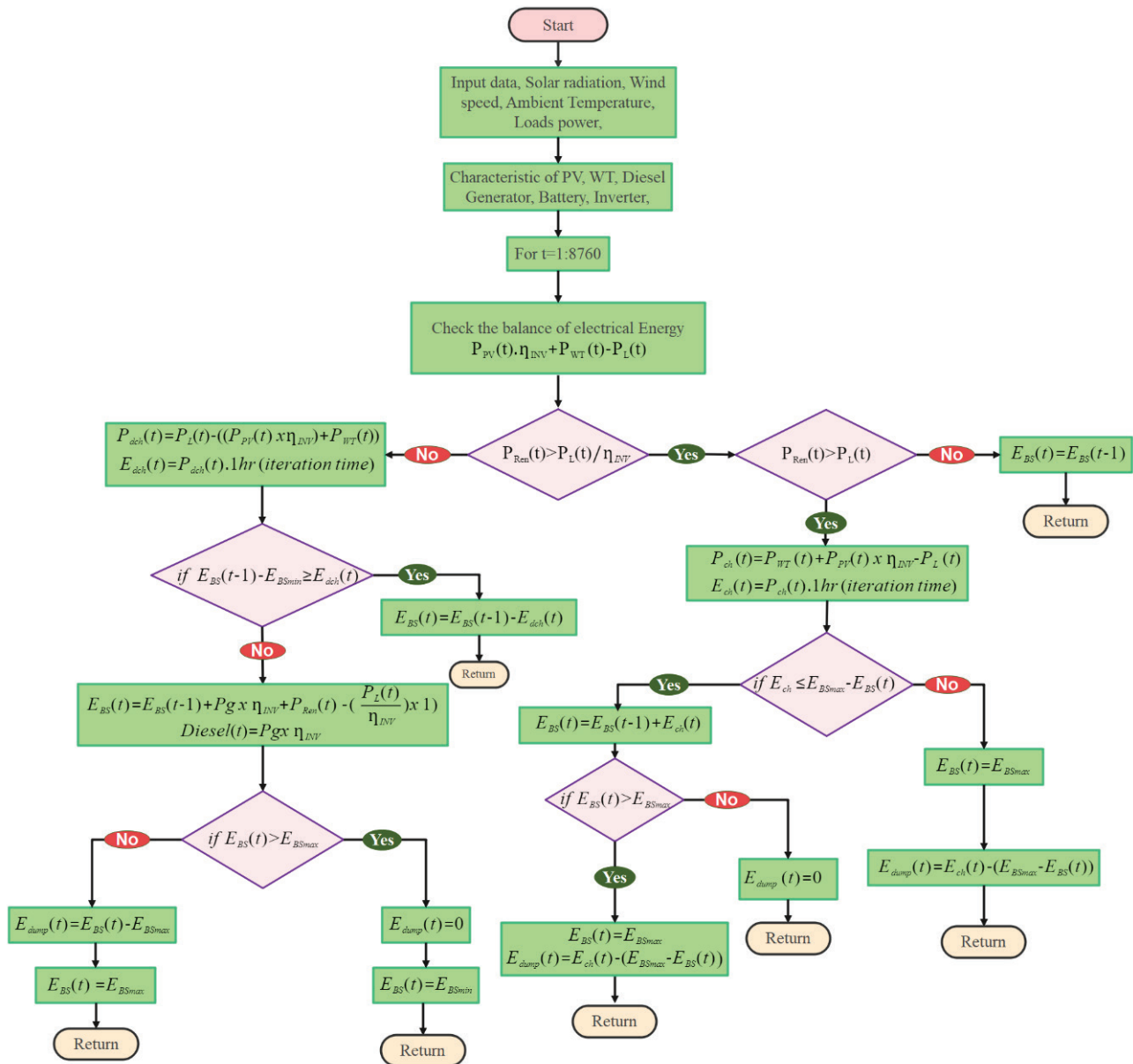


Figure 6. Power management of the PV/WT/DG/BS hybrid energy system.

This calculation considers the comprehensive costs associated with HRES components, which include installation, operation, maintenance, and decommissioning expenses. The LCOE is determined by dividing these combined costs by the total energy produced, as illustrated in Equation 13 [43].

$$LCOE = \frac{C_{ann_total}}{\sum_{t=1}^{8760} E_p} \quad (13)$$

The variable C_{ann_total} denotes the total annual cost in dollars, while E_p represents the total energy production for a year. The C_{ann_total} variable includes the cost of installing photovoltaic panels and a wind turbine, as well as the cost of a diesel generator, battery storage units, and converters [44].

$$C_{ann_total} = C_{ann}^{PV} + C_{ann}^{WT} + C_{ann}^{BSS} + C_{ann}^{DG} + C_{ann}^{Inv} \quad (14)$$

C_{ann}^{PV} , C_{ann}^{WT} , C_{ann}^{BSS} , C_{ann}^{DG} and C_{ann}^{Inv} are the annual costs of PV panels, wind turbines, battery storage units, diesel generators, and bidirectional inverters, respectively.

$$C_{ann}^{PV} = C_{ann,cap}^{PV} + C_{ann,rep}^{PV} + C_{ann,O\&M}^{PV} - C_{ann,SV}^{PV} \quad (15)$$

$$C_{ann}^{WT} = C_{ann,cap}^{WT} + C_{ann,rep}^{WT} + C_{ann,O\&M}^{WT} - C_{ann,SV}^{WT} \quad (16)$$

$$C_{ann}^{BSS} = C_{ann,cap}^{BSS} + C_{ann,rep}^{BSS} + C_{ann,O\&M}^{BSS} - C_{ann,SV}^{BSS} \quad (17)$$

$$C_{ann}^{DG} = C_{ann,cap}^{DG} + C_{ann,rep}^{DG} + C_{ann,O\&M}^{DG} - C_{ann,SV}^{DG} \quad (18)$$

$$C_{ann}^{Inv} = C_{ann,cap}^{Inv} + C_{ann,rep}^{Inv} + C_{ann,O\&M}^{Inv} - C_{ann,SV}^{Inv} \quad (19)$$

$C_{ann,cap}^{PV}$, $C_{ann,cap}^{WT}$, $C_{ann,cap}^{BSS}$, $C_{ann,cap}^{DG}$ and $C_{ann,cap}^{Inv}$ represent the annualized capital costs of PV, WT, BS, DG, and bidirectional inverters, respectively. $C_{ann,rep}^{PV}$, $C_{ann,rep}^{WT}$, $C_{ann,rep}^{BSS}$, $C_{ann,rep}^{DG}$ and $C_{ann,rep}^{Inv}$ are the annual replacement costs of PV, WT, BS, DG, and bidirectional inverters, respectively. $C_{ann,O\&M}^{PV}$, $C_{ann,O\&M}^{WT}$, $C_{ann,O\&M}^{BSS}$, $C_{ann,O\&M}^{DG}$ and $C_{ann,O\&M}^{Inv}$ are the annual operation and maintenance costs of PV, WT, BS, DG, and bidirectional inverters, respectively. $C_{ann,SV}^{PV}$, $C_{ann,SV}^{WT}$, $C_{ann,SV}^{BSS}$, $C_{ann,SV}^{DG}$ and $C_{ann,SV}^{Inv}$ are the salvage value of PV, WT, BS, DG, and bidirectional inverters, respectively.

Loss power supply probability (LPSP)

To ensure the reliability of an HRES, the probability of power supply loss (LPSP) must be considered. LPSP arises when the generated energy cannot satisfy the load demand, leading to a power outage. The value of LPSP ranges from 0 to 1. A value of 0 implies a guaranteed load supply, whereas 1 suggests a complete failure to meet the load. Equation (20) calculates the LPSP over a specific timeframe, T, which is 8760 h [45].

$$LPSP = \frac{\sum_{t=1}^{8760} P_{load}(t) - P_{PV}(t) - P_{WT}(t) + P_{DG}(t) + E_{BSmin}(t)}{\sum_{t=1}^{8760} P_{load}(t)} \quad (20)$$

In this context, $P_{WT}(t)$ denotes the energy produced by the wind turbine at time t. Meanwhile, $P_{PV}(t)$ signifies the power generated by the PV system during that same moment, and $P_{DG}(t)$ illustrates the energy emanating from the diesel generator at time t. $P_{load}(t)$ highlights the electrical consumption at that interval, while $E_{BSmin}(t)$ designates the lowest allowable energy storage level in the battery system. The situation outlined in Equation (21) is also factored into the reliability considerations. In this scenario, the LPSP metric is initialized to zero before running the simulation.

$$P(t)_{load} > P(t)_{generation} \quad (21)$$

Renewable energy factor (REF)

Several metrics were used to assess the integration of RES within an HRES. Equation (22) is used to calculate the REF value when the HRES system incorporates a diesel generator. REF was chosen specifically to minimize the reliance on non-RES components.

$$REF(\%) = \left(1 - \frac{\sum_{t=1}^{8760} P_{DG}(t)}{\sum_{t=1}^{8760} P_{PV}(t) + P_{WT}(t)}\right) \times 100 \quad (22)$$

In the given formula, $P_{DG}(t)$ signifies the energy output from the diesel generator. Conversely, $P_{PV}(t) + P_{WT}(t)$ depicts the energy provided to the load at the specific time interval t. To amplify the REF, it is essential to minimize the latter part of this formula. It is worth noting that the REF has an upper limit set at 100%. Thus, during optimization

efforts, the REF should consistently stay below the benchmark value (ε_{REF}), as highlighted in Equation (23) [46]

$$REF(\%) \leq \varepsilon_{REF} \quad (23)$$

Greenhouse Gas Emission Optimization Model

In the design of an HRES, accounting for greenhouse gas emissions (GHG) is paramount. Systems that emit substantial numbers of GHGs can pose significant environmental risks. The diesel generator within this system is the chief contributor to gas emissions, producing three distinct gasses: CO₂, SO₂, and NO_x. Equation (24) is employed to determine the total gas emissions (TGE) of the system [47]:

$$TGE = \sum_{t=1}^{8760} \left((a_{CO_2} + a_{SO_2} + a_{NO_x}) \times P_{DG}(t) \right) \quad (24)$$

In this study, emission factors of 697, 0.5, and 0.22 were used for CO₂, SO₂, and NO_x, respectively.

Dump Energy Evaluation

In the optimization process, the algorithms reduce the energy spent during discharge. Energy discharge is typically undesirable because it represents energy consumption, especially when there is an overproduction of renewable energy and the battery is at full capacity. To counteract this discharge, energy can be channeled to discharge loads such as campus irrigation, pumping systems, or three-phase resistors. This study leverages an optimal system design to reduce the amount of discharged energy. To compute the cumulative discharge load energy over the system's lifespan, Equation (25) is invoked [48]:

$$D_{total} = \sum_{t=1}^{8760} (E_{WT}(t) + E_{PV}(t) - \frac{E_{Load}(t)}{\eta_{Inv}}) \quad (25)$$

Design Variables

Equation (26) delineates the upper and lower constraints of the decision variables, including the power from wind turbines, solar panels, and battery count.

$$\text{Decision variables} = \begin{cases} 0 \text{ kW} \leq R_{WT} \leq 10000 \text{ kW} \\ 0 \text{ kW} \leq R_{PV} \leq 10000 \text{ kW} \\ 0 \text{ kW} \leq R_{BS} \leq 10000 \text{ kW} \end{cases} \quad (25)$$

The power generated by a wind turbine is represented as R_{WT} . R_{PV} denotes the power generated by solar panels, while R_{BS} signifies the number of batteries. Given the multitude of variables and the intricate nature of the search space, setting boundary values for decision variables in the optimization process is challenging. Typically, these values are determined through trial and error. However, in this study, the HOMERPro software was used to determine the lower and upper boundary values for the algorithms. To ensure swift convergence of the algorithms to the optimal solution, the values from Equation (26) were employed.

Table 2. Optimal sizing results obtained using HOMER Pro under Scenarios 1, 2, 3, and 4 of the proposed HRES

Scenarios	Structure				Cost					
	PV (kW)	WT (kW)	DG (kW)	BS (Quantity)	Converter (kW)	TNPC (\$)	LCOE (\$/kWh)	O&M (\$/Year)	Initial Capital (\$)	REF (%)
Scenario2 (PV+WT+BS)	6,243	15	-	755	1,279	11.6M	0.191	411,642	4.88M	100
Scenario 3 (PV+DG+BS)	15,672	-	1,500	384	1,602	28.3M	0.467	1.06M	11.2M	99.9
Scenario 4 (PV+WT+DG+BS)	10,635	1,583	1,500	384	1,465	26.2M	0.432	933,437	11M	99.99

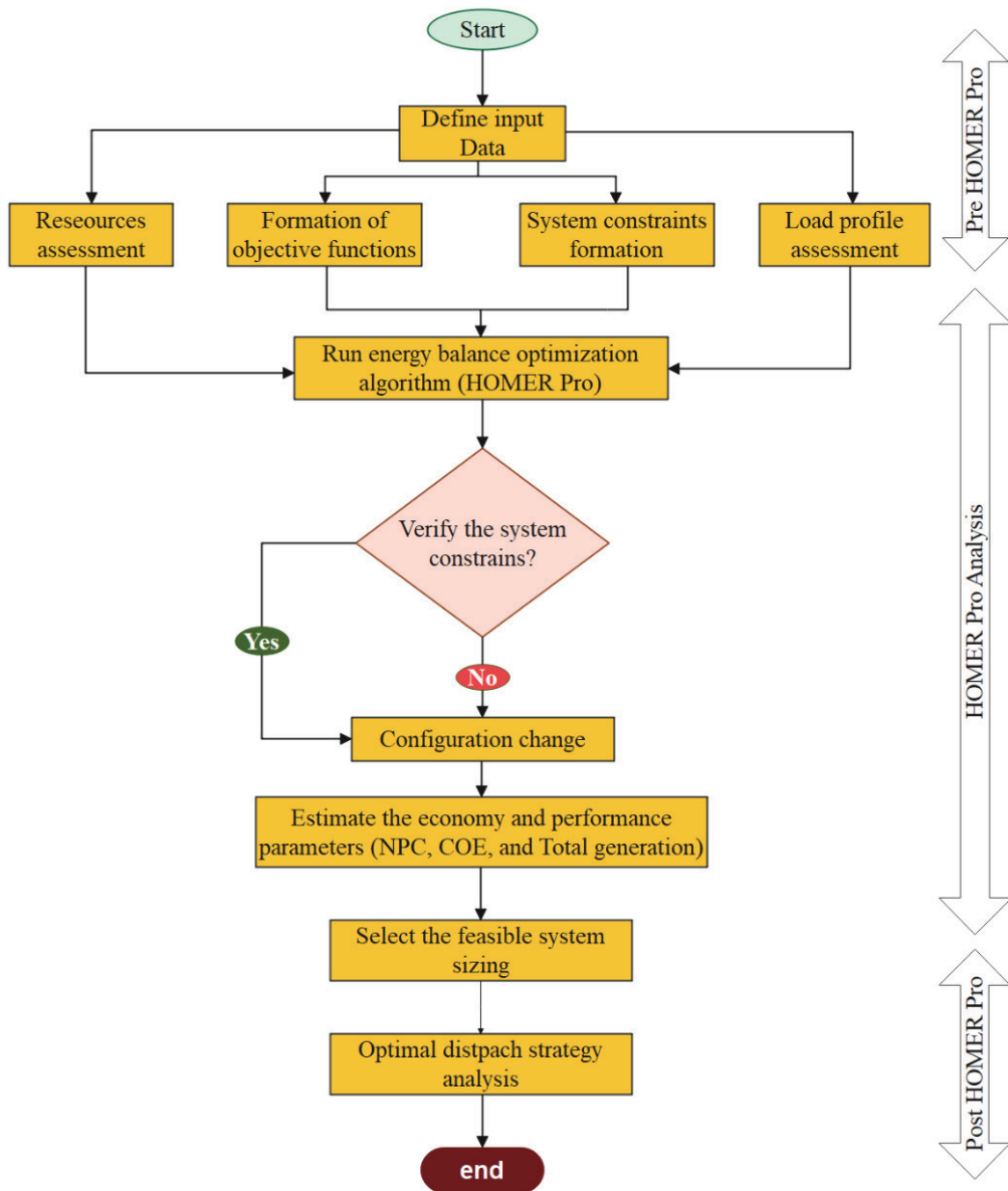


Figure 8. HOMER Pro optimization flow diagram.

surroundings, forage for food, and protect themselves from threats. This behavior is emulated through the principles of information sharing and social cognitive intelligence. In essence, PSO combines individual experiences with group lessons to effectively model complex problems. In the algorithm, a ‘swarm’ is composed of multiple particles. Each of these particles adjusts its position on the basis of both its individual experiences and the collective experiences of its peers. Each particle tracks of its coordinates in the solution space, which correspond to the highest fitness value it has ever attained. This is termed its “personal best” or “pBest.” Moreover, the algorithm acknowledges the best fitness value attained by any particle in the swarm, which is designated as the “global best” or “gBest” [50]. The pseudocode for the PSO algorithm is shown in Figure 9.

Genetic algorithm (GA)

Genetic algorithms (GA) employ heuristic techniques to address intricate problems, making them versatile tools across a wide array of disciplines. The GA approach excels at optimization and is capable of deriving insights from any dataset. It constructs a population of potential solutions using genetic operators such as crossover and mutation on each solution space point, each represented by a genetic parameter termed a chromosome. With each reproductive cycle, the population evolves to include members superior to their predecessors. John Holland, a psychologist and computer scientist at the University of Michigan, pioneered the foundational concepts of genetic algorithms. The core philosophy of genetic algorithms echoes the principle of natural selection: superior generations prevail

while weaker generations fade away. This philosophy is inherently inspired by the evolutionary processes observed in living organisms. Holland articulated his research insights in his 1975 publication, “Adaptation in Natural and Artificial Systems.” Consequently, the algorithm he described became widely recognized as a GA [51]. Genetic algorithms are conceptualized based on the tenet of natural selection, emphasizing the survival and evolution of the fittest solutions. They harness operators such as recombination and mutation to spawn new solutions, while a fitness function gauges the efficacy of these solutions. A hallmark of genetic algorithms is their ability to concurrently evaluate a plethora of solutions, permitting the curation of the most optimal ones from an expansive selection and sidelining the subpar candidates. Consequently, the quality of the solutions procured via genetic algorithms demonstrates a progressive enhancement over iterations.

A strength of genetic algorithms lies in their compatibility with multi-objective optimization techniques. This trait renders them particularly adept at tackling intricate challenges, allowing for the swift identification of optimal solutions. Nonetheless, the intricacies of genetic algorithms might prove challenging for many end users to grasp. Moreover, problem-solving with these algorithms and discerning the most suitable crossover strategies can present difficulties. The pseudocode for GA is shown in Figure 10.

In this pseudocode, P represents the population of individuals and N represents the population size. The algorithm begins by generating an initial population of N individuals

```

Initialize particles randomly within the search space
Initialize particle velocity randomly within a predefined range
Find the fitness value of each particle

Set pBest to the particle's current position for each particle
Set gBest to the position of the particle with the best fitness

While stopping criterion is not met do
  For each particle do
    Update the particle's velocity using the formula:
      velocity = inertia * velocity
      + cognitive component * random(0,1) * (pBest - current position)
      + social component * random(0,1) * (gBest - current position)
    Update the particle's position using the formula:
      position = position + velocity
    Evaluate the fitness value of the new position
    If the new position is better than the particle's pBest, set pBest to the new position
    If pBest is better than gBest, set gBest to pBest
  End For
End While

Return gBest

```

Figure 9. PSO algorithm pseudocode.

```

Initialize population P with N individuals
Evaluate the fitness of each individual in P
While termination criteria not met do:
  Create a new population P'
  While size of P' is less than N do:
    Select two parents from P using a selection method
    Generate offspring by applying crossover and mutation operators to the
    parents
    Evaluate the fitness of the offspring
    Add the offspring to P'
  Replace P with P'
End While
Return the best individual in P

```

Figure 10. GA algorithm pseudocode.

and then evaluates the fitness of each individual in the population.

The algorithm then enters a loop that continues until some termination criteria are met (e.g., a maximum number of generations is reached, or the fitness of the best individual in the population exceeds a certain threshold). In each iteration of the loop, a new population P' is created by selecting two parents from the current population P , generating an offspring by applying crossover and mutation operators to the parents, and evaluating the fitness of the offspring. This process continues until P contains N individuals.

Finally, the current population P is replaced with the new population P' , and the loop continues. The algorithm returns the best individual in the final population P .

Gravity Search Algorithm (GSA)

The gravitational search algorithm (GSA) is a heuristic search method influenced by both population dynamics and the principles of physics, specifically mass interactions. Proposed by E. Rashedi and colleagues in 2009 [52], the GSA draws its inspiration from Newton's law of gravity—a cornerstone of physical theories.

According to Newton's law, every particle in the universe exerts an attractive force on every other particle. This force is directly proportional to the product of their masses and inversely proportional to the square of the distance separating them. In the GSA framework, this concept is translated to agents, each having a mass that corresponds to fitness function values. As the algorithm progresses over iterations, these masses attract each other because of their inherent gravitational forces. The heavier a mass—indicative of its proximity to the global optimum—the stronger its gravitational pull. As a result, these dominant masses attract other masses on the basis of their relative distances, guiding the algorithm's masses to gravitate toward the

heaviest, most optimal solution while exerting influence on their neighbors.

As a population-based method, GSA treats candidate solutions as individual masses. Each solution or mass functions like a particle. These particles navigate the search space, influenced by gravitational dynamics shaped by fitness functions. GSA's versatile nature has found applications across various optimization domains, including vehicle routing, artificial neural networks, energy systems, and medical applications [53]. For a step-by-step breakdown of the algorithm, one can refer to Figure 11, which provides the GSA pseudocode.

Partical Swarm Optimization Gravity Search Algorithm (PSOGSA)

The particle swarm optimization gravity search algorithm (PSOGSA) is a hybrid optimization algorithm that combines the strengths of PSO and GSA to address intricate optimization challenges. While PSO mirrors the social behaviors of bird swarms, GSA emulates the gravitational interactions between celestial bodies. Together, they offer an effective approach to pinpointing the global optimum within a search space. In PSOGSA, a population of particles traverses the search space to identify the most suitable solution. Each particle receives a fitness score. This score steers the search toward the most promising solutions. Particles modify their trajectories on the basis of the PSO algorithm. They adjust their velocities and positions using both their personal experiences and the collective knowledge of the swarm. Subsequently, GSA refines the solutions derived from PSO by emulating the gravitational interactions among particles. This iterative process fine-tunes each solution, urging particles toward the global optimum. The combination of PSO and GSA fosters a more comprehensive and effective exploration of optimal outcomes. PSOGSA is a versatile algorithm. Its effectiveness has been

Input:

- **n**: number of agents
- **m**: number of iterations
- **ub**: upper bounds of decision variables
- **lb**: lower bounds of decision variables
- **function**: objective function to optimize

Output:

- **best_agent**: the best solution found by the algorithm
- **best_fitness**: the objective function value of the best solution found

Initialize:

- Define the gravitational constant G
- Define the damping factor α
- Initialize agents randomly within the search space
- Evaluate the fitness of each agent
- Set the **best_agent** to be the agent with the best fitness value
- Set the **best_fitness** to be the **best_agent**'s fitness value

for i in range(m):

 for j in range(n):

Calculate the mass of the current agent

$mass_j = mass_calculation(agent[j].fitness, best_fitness)$

Calculate the force acting on the current agent

$force_j = force_calculation(agent[j], best_agent, G)$

Update the velocity and position of the current agent

$velocity_j = velocity_calculation(agent[j], force_j, mass_j, \alpha)$

$position_j = position_update(agent[j], velocity_j, ub, lb)$

Evaluate the fitness of the new position

$fitness_j = evaluate_fitness(position_j, function)$

Update the **best_agent** and **best_fitness** if the new fitness value is better

 if $fitness_j < best_fitness$:

$best_agent = position_j$

$best_fitness = fitness_j$

Update the gravitational constant and damping factor for the next iteration

$G = G_update(G, i, m)$

$\alpha = \alpha_update(\alpha, i, m)$

Return:

- **best_agent**
- **best_fitness**

Figure 11. GSA algorithm pseudocode.

demonstrated in diverse domains such as engineering, finance, and medicine. This highlights its ability to solve complex optimization problems [54].

PSO and GSA are both potent optimization techniques. This study introduces a unique approach by integrating them through what we term a “low-level co-evolutionary heterogeneous hybrid approach.” Unlike traditional

methods, where algorithms operate sequentially, our hybrid strategy runs PSO and GSA simultaneously. This heterogeneous approach employs two separate algorithms to derive superior results. At the heart of PSOGSA is the blend of the social cognition attributes of PSO, as demonstrated by “gbest,” and the adept local search capabilities of GSA. The update mechanism in PSOGSA heavily weighs the quality

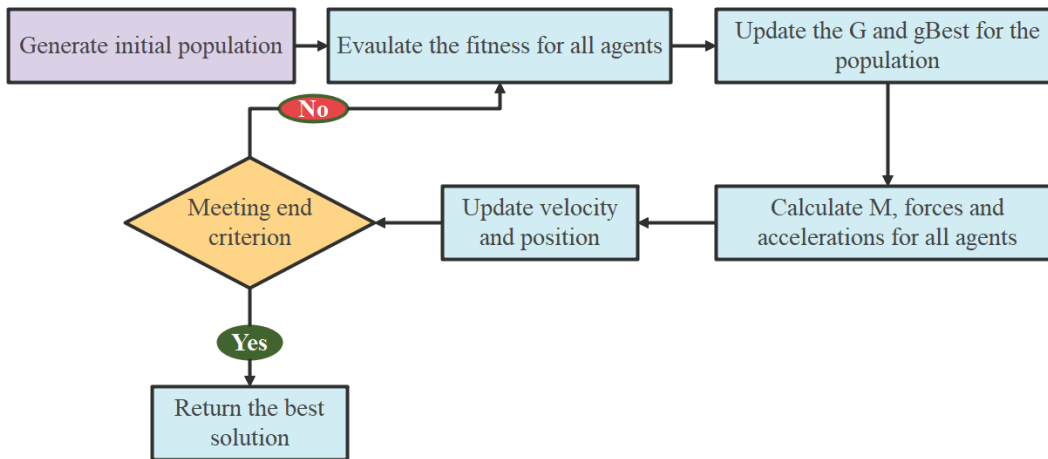


Figure 12. Implementation steps of the PSO-GSA algorithm.

of the solutions. Thus, agents nearing the most promising solutions magnetically pull other agents operating in the same region. This attraction ensures that agents slow down as they close in on a potential solution, thereby preventing any oversight. Additionally, by integrating “gBest,” each agent can draw upon the most effective solution identified thus far [55].

A comprehensive outline of the PSO-GSA process is shown in Figure 12.

Genetic Algorithm Partial Swarm Optimization (GAPSO) Approach

As illustrated in Figure 13, the GAPSO algorithm begins by determining a specific number of iterations for a random population and then generating a parameter. The GA algorithm is subsequently applied to this initialized population for half of the determined iterations, creating multiple solutions for the population scaling issue. For instance, if the total number of iterations is n , the GA algorithm would execute $n/2$ times. This approach is supported by the findings of Alajmi and Wright [56]. To gauge the efficiency of the algorithm, several test runs were conducted, after which the parameter values were adjusted. These tests suggest that the GAPSO algorithm achieves its best performance when the iterations are evenly divided between the PSO and GA algorithms.

Numerous researchers have explored multi-objective optimization challenges in HRES applications using different target metrics. Bates and Granger [57] pioneered the introduction of GAPSO, asserting that a combined forecast model of two distinct types surpassed individual models. Pesaran et al. [58] adopted GA and PSO metaheuristic algorithms for forecasting in the electricity sector and determined that the PSO-driven exponential model was the most effective. Meanwhile, Unler [59] developed a PSO-centric demand forecasting model for Turkey that incorporated gross domestic product and population projections. Younes M. et al. [60] used the GAPSO hybrid method to address economic distribution challenges.

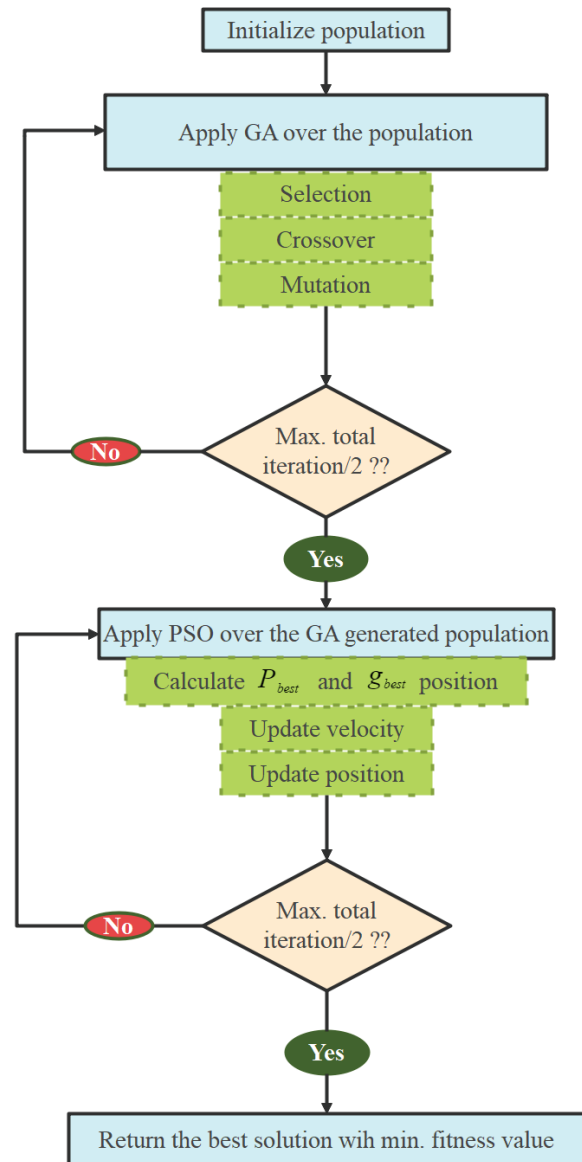


Figure 13. Flow chart of the GAPSO algorithm.

This study models the HRES sizing challenge using the GAPSO algorithm, factoring in available resources. When there is a high iteration count, GA-based algorithms generally outperform their counterparts. However, as the number of iterations increases, the GA algorithm takes longer to converge to an optimal solution. On the other hand, PSO-based algorithms are lauded for their speed and efficiency. However, the swift convergence of PSO-based algorithms can sometimes lead them to settle at a local optimum, possibly skewing the results [61]. The proposed GAPSO method combines the strengths of both the PSO and GA algorithms. When compared with other similar algorithms, GAPSO is anticipated to be more efficient. Moreover, the integration of the GA mutation operator in GAPSO counters the risk of settling at local optima, thus enhancing solution accuracy.

RESULTS AND DISCUSSION

With a focus on minimizing the ACS of the HRES, this study aims to optimize the HRES economically using GA, PSO, GSA, GAPSO, and PSO-GSA algorithms. The PV/WT/BS/DG system considers several constraints, including the battery state of charge (SOC), optimal system sizing, and ensuring reliable electricity demand fulfillment. The

algorithms applied in the optimization process were developed in the MATLAB environment. Only an LPSP value of 0% was used for simulation, indicating that the energy requirement was fully met. All pertinent data and factors associated with hybrid systems and RES, including wind and solar energy, load values, temperature, battery size, depth of charge, and type, were integrated.

In addition to the proposed GAPSO algorithm, four other algorithms — PSO-GSA, PSO, GSA, and GA — were developed and applied to address the microgrid system design challenge. This approach was used to verify the reliability and effectiveness of the hybrid algorithm in determining the optimal size of the stand-alone hybrid microgrid system. The results were juxtaposed with those generated by the GAPSO algorithm, and Figure 19 illustrates the convergence behavior of the algorithms for various off-grid microgrid control parameters. The ACS value consistently declined during the iteration process, which affirms that the optimization was directed toward the perfect system size. Therefore, any reduction in the objective function was deemed crucial because it further elucidated the optimal size. A meticulous analysis of the convergence behavior of the different algorithms, targeting the ideal configuration of a hybrid microgrid system, demonstrated that GAPSO streamlines the process efficiently,

Table 2. Optimal sizing results obtained with PSO, GA, GSA, GSAPSO, and GAPSO

Outputs	GA	PSO	GSA	PSOGSA	GAPSO
Execution time (sec)	334.71	21.57		528.73	658.14
Wind turbines (kW)	0	0	0	0	0
Solar power (kW)	3,743.62	3,559.11	3,600.36	4,475.55	3,640.86
Battery storage power (kW)	4,645.94	4,874.34	5,127.03	3,775.55	4,767.55
Total wind energy (kWh)	0	0	0	0	0
Total solar energy (kWh)	5,642,656.27	5,364,553.17	5,426,720.70	6,745,881.42	5,487,772.63
Total diesel generator	0	0	0	0	0
Energy generation (kWh)					
Wasted energy (kWh)	1,867,404.01	1,606,380.84	1,664,568.55	2,904,329.17	1,721,714.38
Total load demand (kWh)	3,730,393.65	3,730,393.65	3,730,393.65	3,730,393.65	3,730,393.65
Total gas emission (TGE)	0	0	0	0	0
Battery storage input energy (kWh)	2,053,235.75	2,053,235.75	2,051,539.83	2,071,692.96	2,052,141.97
Battery storage output energy (kWh)	2,204,197.12	2,204,197.12	2,215,601.32	2,156,354.34	2,212,297.34
LCOE (\$/ kWh)	0.1801	0.1800	0.1859	0.1811	0.1800
TNPC (\$)	10,907,327.57	1,0902,623.70	1,1256,179.50	10,967,366.70	10,898,221.74
REF (%)	100	100		100	100
Annual cost of system (\$)	672,035.63	671,746.01	693,514.66	675,732.28	671,474.98
Wind cost (\$)	0	0	0	0	0
Solar cost (\$)	5,473,458.48	5,203,694.44	5,263,997.85	6,543,602.89	5,323,219.11
DG cost (\$)	0	0		0	0
Battery cost (\$)	5,391,721.42	5,656,781.58	5,950,033.98	4,381,616.13	5,532,854.96
Inverter cost (\$)	42,147.66	42,147.66	42,147.66	42,147.66	42,147.66

thus minimizing computational time and resource usage, while yielding superior outcomes. As delineated in Table 3, GAPSO is the most economical solution compared with the other algorithms. The annual cost of the HRES via GAPSO is \$671,474.98, accompanied by an LCOE value of \$0.180. The optimized system encompasses 3,640.86 kW of PV and 4,767.55 kW of BS, contributing an additional 1,743,197.2546 kWh of energy that could either be channeled toward campus irrigation or sold to the grid. In summary, the GAPSO algorithm-based optimization methodology provides an effective solution to the intricate microgrid design quandary.

The cost details for a project encompass various factors, including the total initial cost, ongoing maintenance and operating expenses, projected lifespan, and quantities and costs of each component of the hybrid power system. To offer precise solutions in the least amount of time, specialized algorithm designs have been developed. In the proposed system, solar panels and batteries are the sole means that satisfy the overall energy demand. Table 3 presents the optimization results for the GA, PSO, GSA, PSO-GSA, and GAPSO algorithms. For comparative purposes, we have posited a maximum count of 5,000 solar PV panels, 10,000 wind turbines, and 10,000 batteries across all scenarios. The proposed system employs a cycle charging approach, yielding optimal outcomes for the total number of PV panels, WT, and BS.

Figure 14 illustrates the average monthly energy balance over a year. Upon evaluating the HRES, it becomes

clear that the outputs from wind and solar power align well with the available wind and solar resources. During months when PV panels produce less energy—specifically in January, February, November, and December—the batteries step in to supply the necessary electricity. In contrast, the remaining months witnessed a surge in solar energy generation due to enhanced natural resources. Notably, battery bank usage declines during the summer months, leading to decreased power consumption. The chart also indicates that HRES produces surplus energy. The campus uses this additional 1,721,714.38 kWh of energy for irrigation and other functions. Alternatively, it can be fed into the grid or allocated to other systems.

The optimal performance of the proposed HRES was verified over a span of two weeks throughout the year. Figure 15(a) illustrates the third week of June, during which the load is lower, whereas Figure 15(b) represents the second week of January, a period with higher load demand. Both figures demonstrate the weekly power fluctuations among the various system components. In January, the battery’s SOC approaches its minimum charge status, and solar energy generation is diminished compared with other months. Conversely, June is characterized by elevated solar energy output and a battery SOC near its maximum charge status.

The measurement of the battery’s SOC is crucial because it serves as the primary energy storage source for the HRES. Figure 16 illustrates the average monthly changes in the battery’s SOC and the annual energy input and output. The

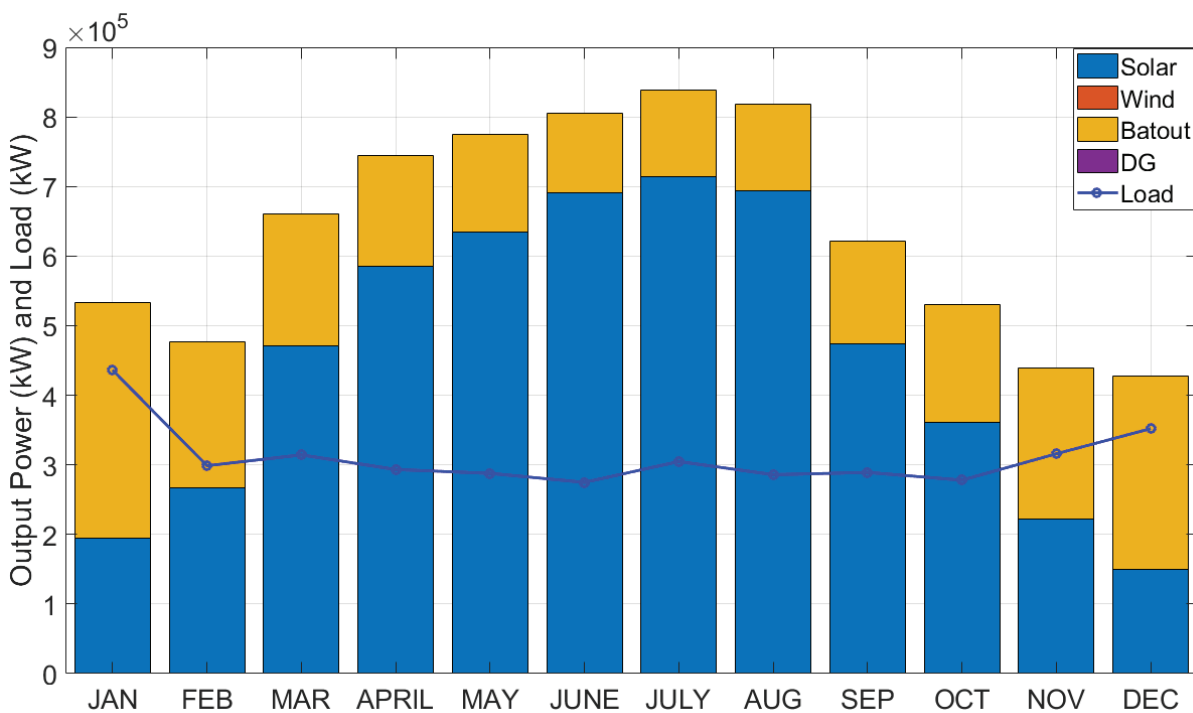


Figure 14. Average monthly energy share to meet load requirements with the stand-alone PV/BS option.

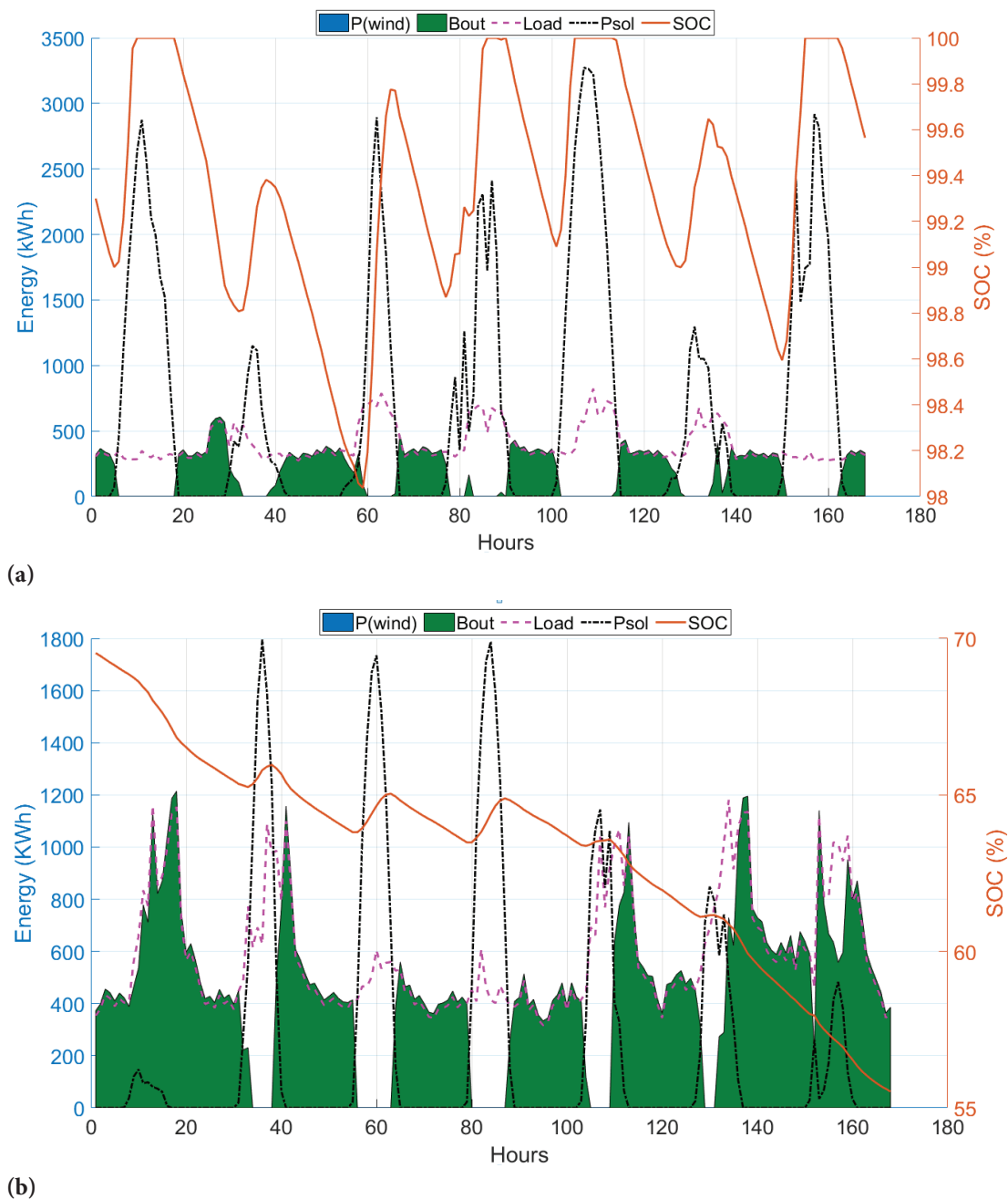
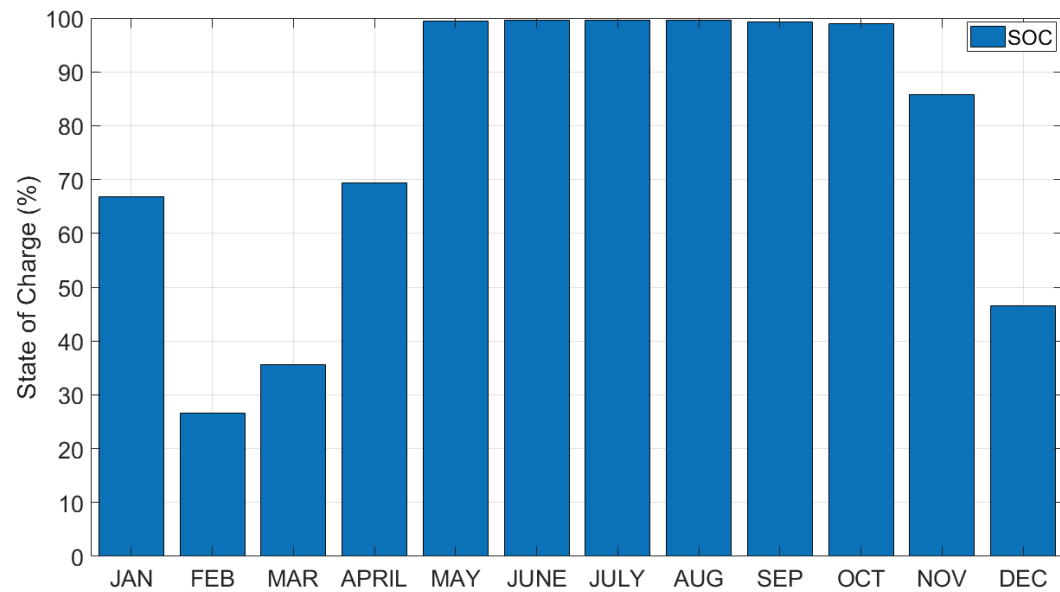


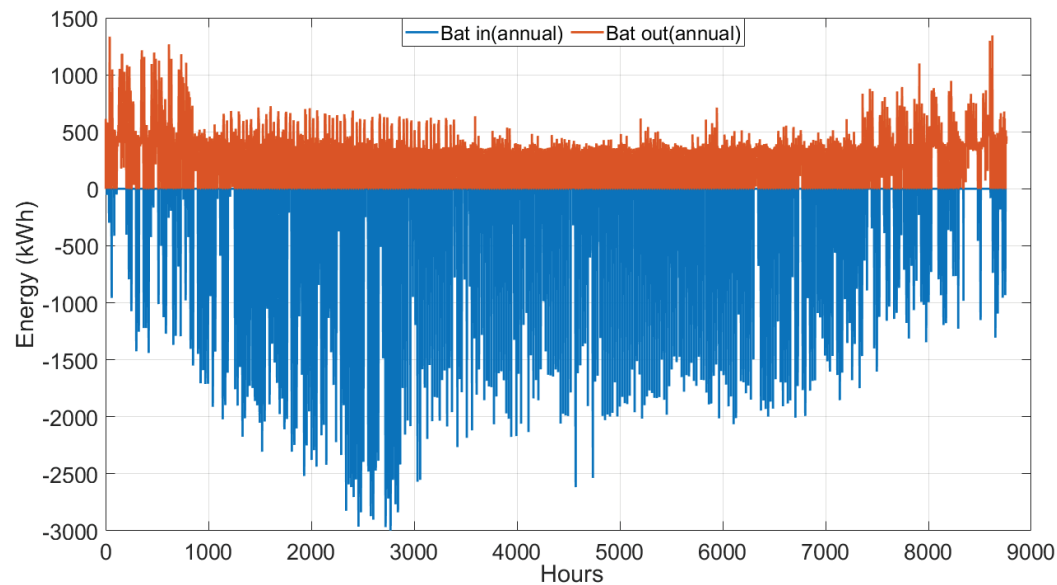
Figure 15. Comparison analysis between the highest and lowest load profiles in 1 year.

predefined initial SOC level and the lowest allowed SOC were 100% and 20%, respectively. Moreover, Figure 16(a) demonstrates that the battery SOC consistently remains within this predetermined range. Figure 16 highlights the typical SOC values during the resource-scarce months of January, February, March, April, and December. Figure 16(b) can be referred to for tracking the energy input-output of the batteries throughout the year. As depicted in the graph, ‘Bat out’ represents the battery discharge. This discharge corresponds to the energy supplied to the load by the battery storage system. On the other hand, ‘Bat in’

indicates the battery charge or excess renewable energy produced once the battery storage system has met the load’s demand. This data is instrumental in monitoring the battery’s performance gaging the energy contributed to or drawn from the system, recognizing energy usage patterns, and making informed decisions on battery charging or discharging to optimize its efficiency. Battery charge rates were as follows: 67.04% in January, 26.62% in February, 34.09% in March, 65.57% in April, 85.57% in November, 46.41% in December, and nearly 100% in the other months.



(a)



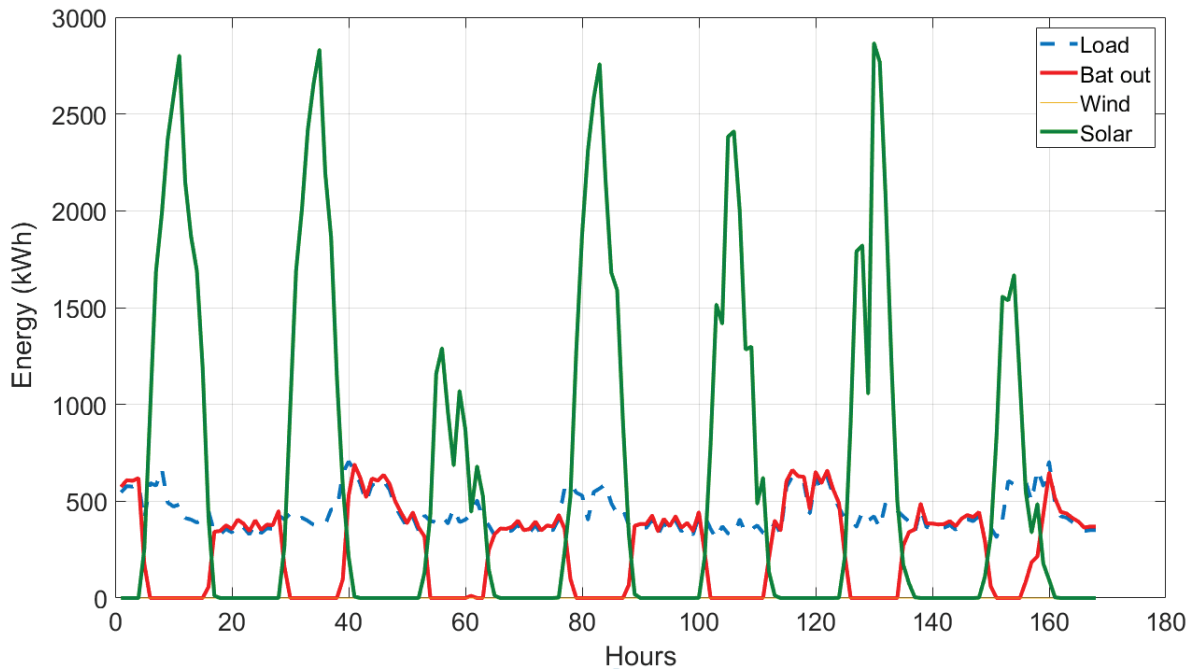
(b)

Figure 16. Battery energy balance (a) Average monthly battery state of charge (%) (b) Annual battery energy balance (kWh).

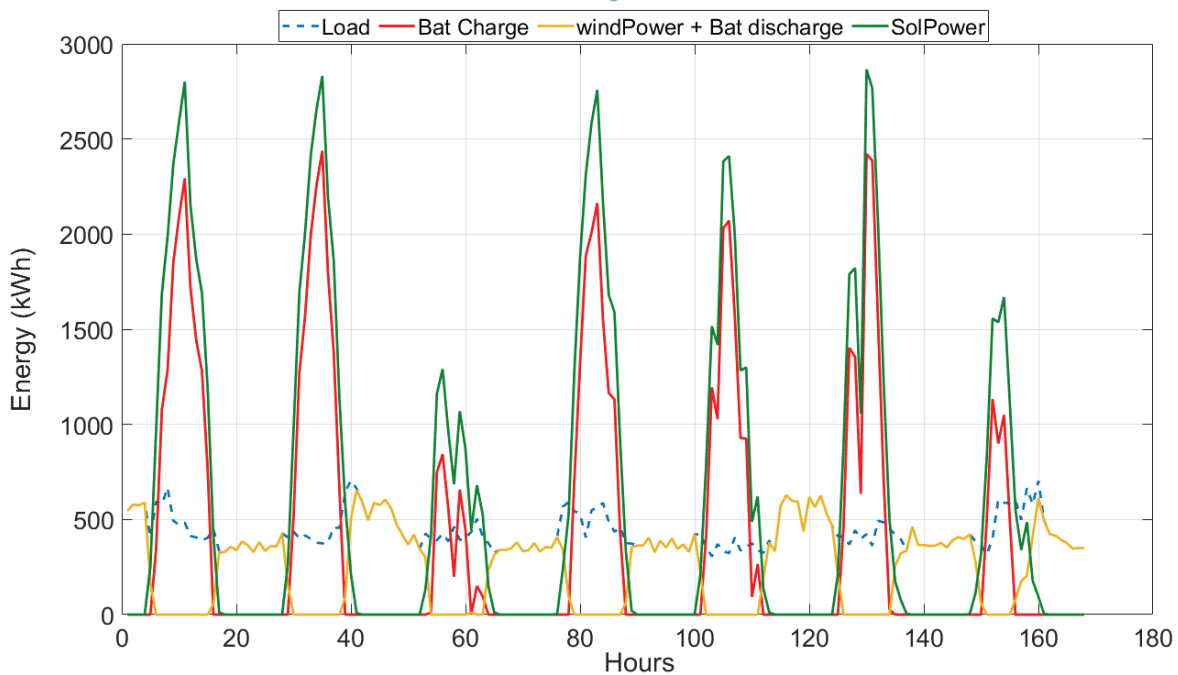
Figure 17 shows the weekly energy values for load, battery discharge, wind, and solar energy. The load is primarily supported by energy sources, including solar, wind, and battery discharge. The operating strategy prioritizes the use of wind and solar energy to cover most of the load. When the renewable energy from the sun and wind is not sufficient to handle the load, the battery discharges. If both the battery bank and the RES are unable to meet the load requirement, the DG supplies the necessary power. Compared with Figure 17(a), Figure 17(b) introduces an

additional line representing battery charging. This scenario depicts the battery being charged both when the RES are generating energy and during times of surplus energy availability, such as when ample solar energy is present.

Figure 18 shows a comparison graph of renewable energy production and load demand. The graph indicates that RES is responsible for the majority of the energy supplied to the load. RES meet the load demand in all months except for January, February, November, and December. The diesel generator is not used throughout the year.



(a)



(b)

Figure 17. HRES optimization balance: (a) load, battery discharge, and wind and solar power; (b) load, battery charge, wind power, battery discharge, and solar energy.

In Figure 19, the impact of changes in converter efficiency on the LCOE and ACS values of the proposed microgrid is displayed, showing an inverse relationship between them. As the efficiency of the inverter increases, both the ACS and LCOE values decrease.

The fitness graphs in Figure 20, specifically parts (a) through (e), along with the PSO, GA, GSA, PSOGSA, and GAPSO algorithms, illustrate the final optimization process. The convergence comparison curve in Figure 21 demonstrates how the algorithms used in the HRES size optimization process progress toward the highest quality

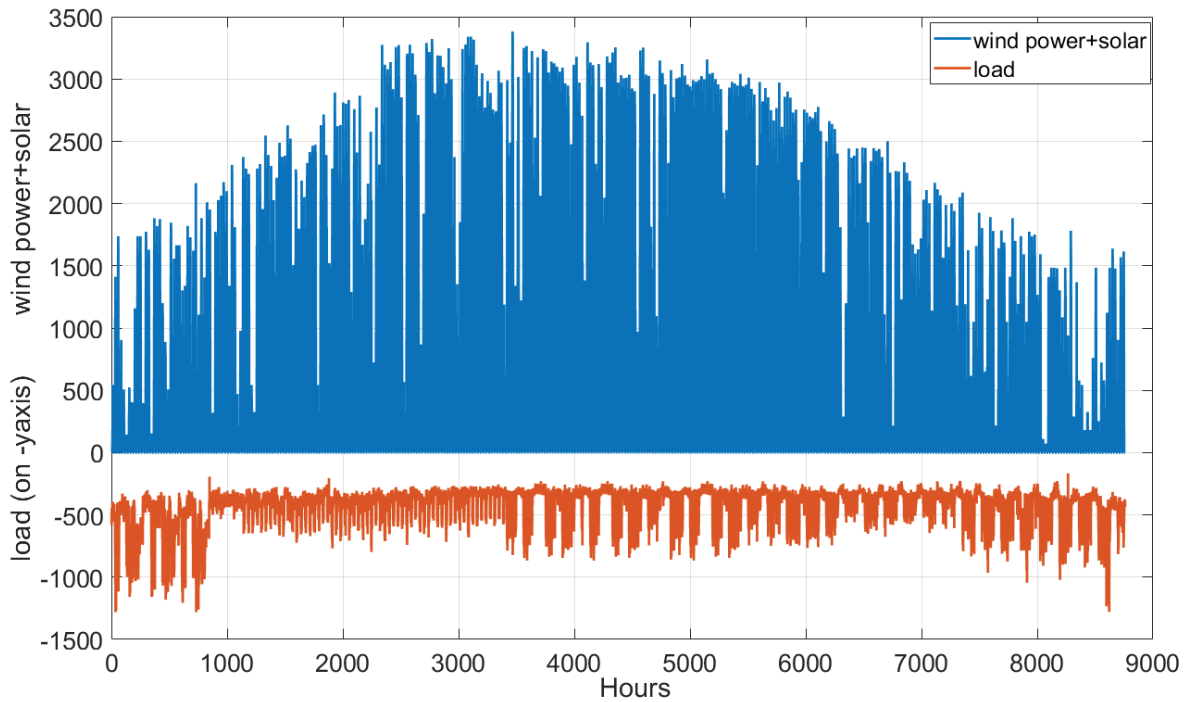


Figure 18. Yearly overview of renewable energy production and consumption demand.

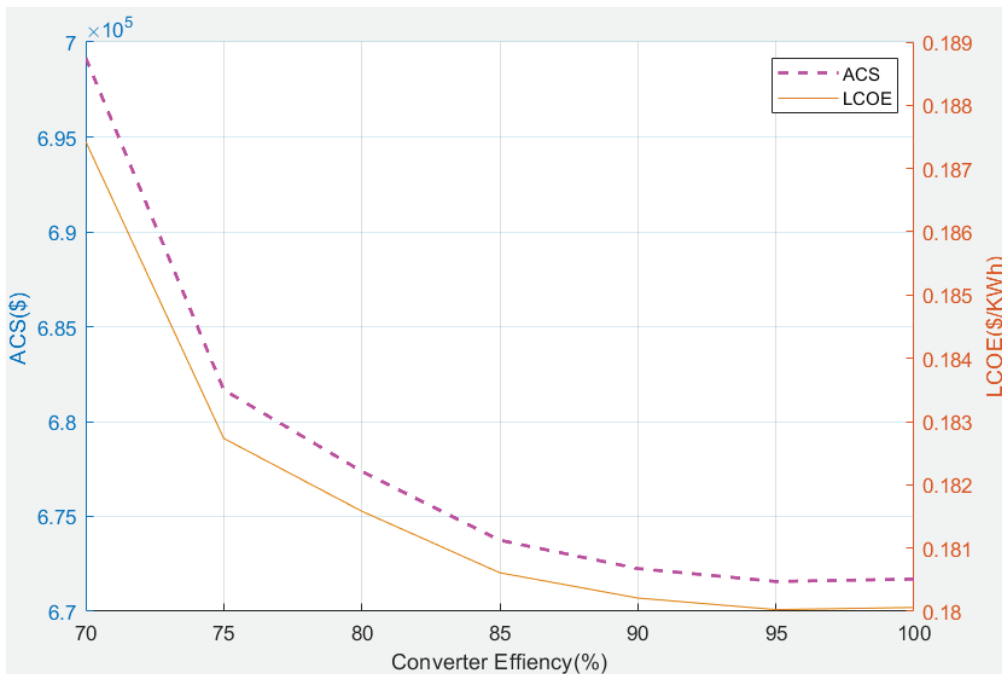


Figure 19. Effect of converter efficiency on the LCOE value.

solution. The shape and slope of the graphs in Figure 21 indicate the speed at which the algorithm approaches the optimal outcome based on the number of optimization iterations. Among the algorithms, the GAPSO algorithm

attains an ACS value of (\$)671,474.98, whereas GSAPSO obtains (\$)675,732.28, GA obtains (\$)672,035.63, GSA obtains (\$)693,514.66, and PSO obtains (\$)671,746.01. Observations indicate that the GAPSO algorithm

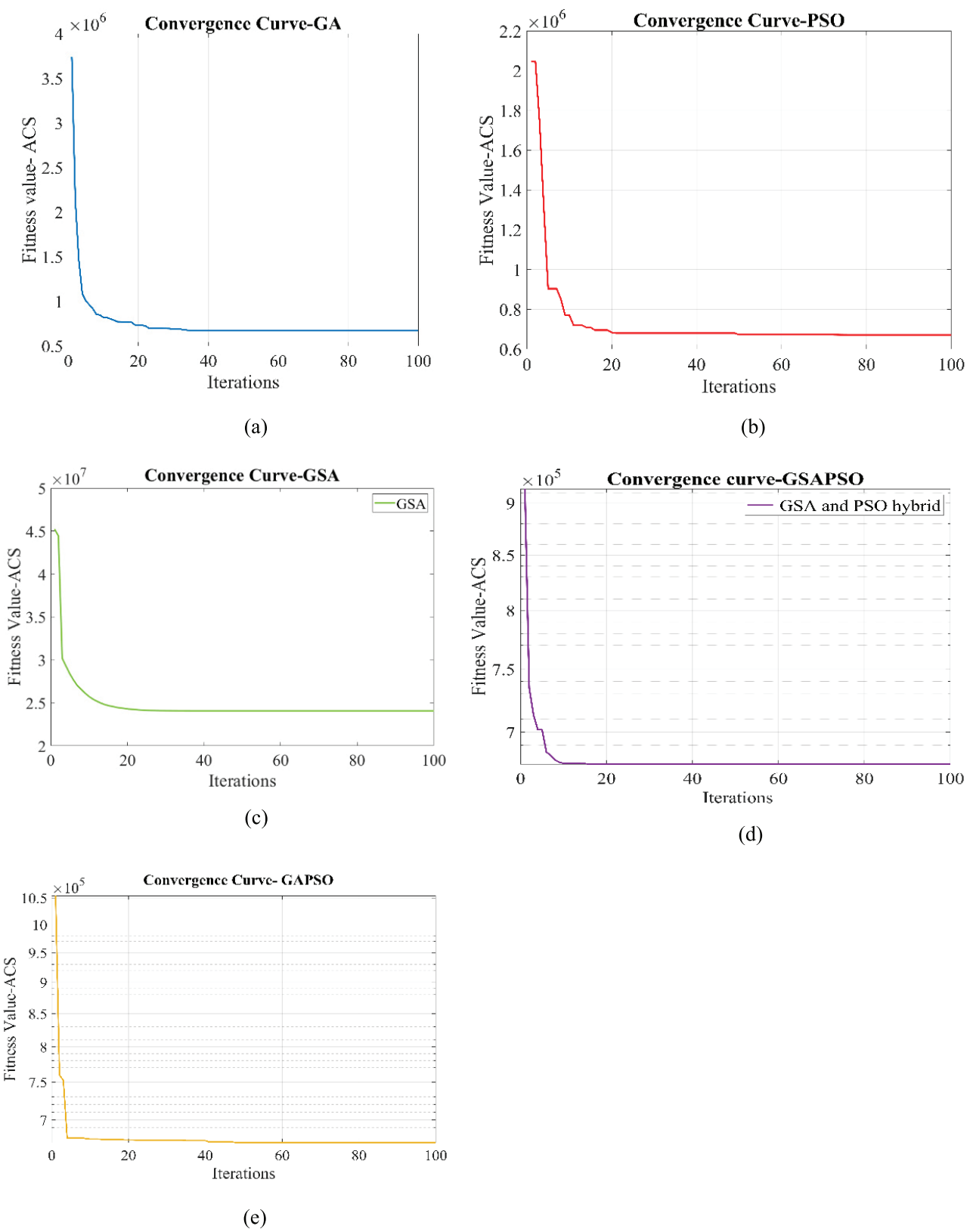


Figure 20. Convergence of GA, PSO, GSA, GSAPSO, and GAPSO algorithms in HRES optimization.

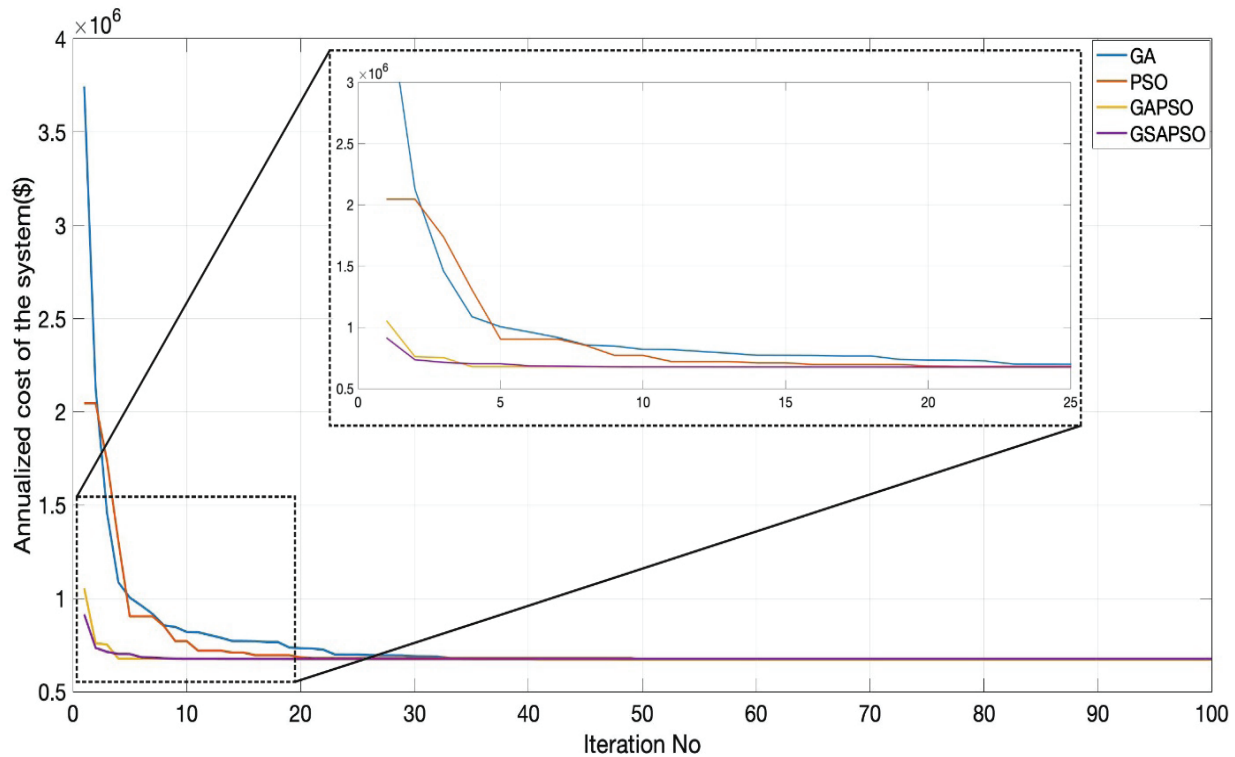


Figure 21. Convergence process of algorithms in the optimal solution of the proposed HRES.

approaches the optimal value quickly after the eighth iteration and yields the solution.

CONCLUSION

In this study, a combination of optimization techniques, including GAPS0, GSAPSO, GA, GSA, and PSO algorithms, was used to determine the optimal sizing of a stand-alone hybrid renewable energy system consisting of PV/WT/BS/DG components for a university campus. The study satisfied the campus' energy needs while minimizing environmental damage and reducing overall annual costs. Hourly load data from the university and information on ambient temperature, wind speed, and solar radiation were used to simulate the system's energy flow with hourly resolution for a full year. Based on the optimization results, the PV-BS components were found to be the most effective. The HOMERPro software was used to verify the sizing approach proposed in the study, which is the industry standard for optimizing microgrid designs. However, the findings of the algorithms produced results that were lower than the leveled energy cost achieved with the HOMERPro software. The optimization strategies of the two versions differed significantly, demonstrating the importance of making informed decisions on the optimization method when evaluating the hybrid system's economic performance and reliability. To balance the use of hybrid algorithms and assessment procedures, the strengths and

benefits of each algorithm were evaluated. Although the algorithms used assessed trends leading to the optimal outcome, the fast-converging GAPS0 algorithm produced superior outcomes. The suggested GAPS0 technique is competitive regarding resolving the HRES sizing problem and is expected to be applied to more challenging issues in future research.

Using the GAPS0 algorithm technique, the optimization results in an ACS value of \$671,474.98, LCOE value of \$0.1800, TNPC value of \$10,898,221.74, and REF value of 100%. These outcomes show that the university campus's load is completely fulfilled while maintaining reasonable costs and minimal environmental impact. The RES provides the required load, rendering the diesel generator, which was initially intended as a backup unit, unnecessary. The environmental benefits of the study are highlighted by the fact that the TGE value is zero. Any excess energy generated by renewable sources can be used for power on-campus energy needs, sold to the grid, or invested in irrigation systems. These findings provide a valuable reference for policymakers and investors in the renewable energy sector.

The developed sizing methodology's key characteristics areas follows:

- The software allows for simulating HRESs that incorporate wind, solar-diesel, and energy storage technologies, enabling the evaluation of the system's economic viability and reliability.

- The dispatch strategy specifies every possible system state as a column in the time series output file, and the resulting delivery plan prioritizes the use of RES.
- It is clear from the designed model that an HRES using only solar panels and batteries can meet the load demand while complying with all restrictions. One could argue that solar energy makes the greatest contribution.
- Using energy graphics that accompany technical results, instant energy analysis results are always visible. The study findings lead us to conclude that the suggested algorithm greatly assists in resolving optimal design issues in HRES.
- The energy analysis graphs and data from the program will enable the evaluation of the specified region from a techno-economic and environmental viewpoint.
- This statement highlights that the feasibility study is innovative and will have a direct impact on avoiding unnecessary investments and promoting the efficient use of public resources.

NOMENCLATURE

Acronyms

ABC	Artificial bee colony
ACS	Annual cost of the system
AEFA	Artificial electric field algorithm
BG	Biogas
BS	Battery storage
BSS	Battery storage system
COE	Cost of energy(\$/kWh)
CRF	Capital recovery factor
CC	Cycle charging
DG	Diesel generator
DOD	Depth of discharge
EMS	Energy management system
ESS	Energy storage system
FLC	Fuzzy logic controller
FPA	Flower pollination algorithm
FC	Fuel cell
GA	Genetic algorithm
GAPSO	Genetic algorithm Particle swarm optimization
GSAPSO	Gravity search algorithm Particle swarm optimization
GSA	Gravity search algorithm
HES	Hydroelectric power plants
HRES	Hybrid renewable energy systems
IGOA	Improved grasshopper optimization algorithm
LCOE	Levelized cost of energy (\$/kWh)
LPSP	Loss of power supply probability
LF	Load following
TNPC	Total net present cost (\$)
PV	Photovoltaics
RES	Renewable energy sources
PSO	Particle swarm optimization
RE	Renewable energy
REF	Renewable energy fraction

SOA	Seagull optimization algorithm
SOC	Battery state of charge value
SOCmax	Battery state of charge (maximum value)
SOCmin	State of charge (minimum value)
TS	Tabu search algorithm
WOA	Whale optimization algorithm
WPS	Wind power plants
WT	Wind turbine

Symbols

$P_{WT}(t)$	Output power of wind turbine at time t (kW)
$P_{PV}(t)$	Output power of photovoltaic panel at time t (kW)
$P_L(t)$	Load energy demand
η_{Inv}	The efficiency of an inverter
$P_{ch}(t)$	Power allocated for charging the battery
$E_{ch}(t)$	Energy charged to the battery
$P_{distch}(t)$	Discharge battery power
$E_{distch}(t)$	Energy is discharged from the battery
$E_p(t)$	Total energy production in a year
$C_{ann,cap}^{PV}$	Annual capital costs of photovoltaic panel
$C_{ann,cap}^{WT}$	Annual operation and maintenance costs of inverter
$C_{ann,cap}^{BSS}$	Annual capital costs of battery storage system
$C_{ann,cap}^{DG}$	Annual capital costs of diesel generator
$C_{ann,cap}^{Inv}$	Annual capital costs of inverter
$C_{ann,rep}^{PV}$	Annual replacement costs of photovoltaic panel
$C_{ann,rep}^{WT}$	Annual replacement costs of wind turbine
$C_{ann,rep}^{BSS}$	Annual replacement costs of battery storage system
$C_{ann,rep}^{DG}$	Annual replacement costs of diesel generator
$C_{ann,rep}^{Inv}$	Annual replacement costs of inverter
E_{BSmin}	Minimum battery energy
E_{BSmax}	Maximum battery energy
$E_{BSS}(t)$	Energy of battery
$E_{dump}(t)$	Energy dumped/wasted
$DG_{hr}(t)$	Diesel generator is running at time t
DG_P	The power produced by diesel generator
O&M	Operation and maintenance
t	Time
σ	The self-discharge rate of the battery
$C_{ann,O\&M}^{PV}$	Annual operation and maintenance costs of photovoltaic panel
$C_{ann,O\&M}^{WT}$	Annual operation and maintenance costs of wind turbine
$C_{ann,O\&M}^{BSS}$	Annual operation and maintenance costs of battery storage system
$C_{ann,O\&M}^{DG}$	Annual operation and maintenance costs of diesel generator
$C_{ann,O\&M}^{Inv}$	Annual operation and maintenance costs of inverter
$C_{ann,SV}^{PV}$	Salvage value of photovoltaic panel
$C_{ann,SV}^{WT}$	Salvage value of wind turbine
$C_{ann,SV}^{BSS}$	Salvage value of battery storage system
$C_{ann,SV}^{DG}$	Salvage value of diesel generator
$C_{ann,SV}^{Inv}$	Salvage value of inverter

AUTHOR CONTRIBUTIONS

Aykut Fatih Güven: Conceptualization, methodology, investigation, writing-original draft, Writing-review-editing, formal analysis, software, resources.

Nuran Yörükeren: Methodology, resources, writing-original draft, investigation, validation.

DECLARATION OF COMPETING INTEREST

The authors declare that they do not have any known competing financial interests or personal relationships that could appear to have influenced the work reported in this paper.

DATA AVAILABILITY

Data available on request due to privacy/ethical restrictions. The data that support the findings of this study are available on request from the corresponding author. The data are not publicly available due to privacy or ethical restrictions.

ETHICS

There are no ethical issues with the publication of this manuscript.

REFERENCES

- [1] Pinto R, Henriques ST, Brockway PE, Heun MK, Sousa T. The rise and stall of world electricity efficiency: 1900-2017, results and insights for the renewables transition. *Energy* 2023;269. [\[CrossRef\]](#)
- [2] Effatpanah SK, Ahmadi MH, Aungkulanon P, Maleki A, Sadeghzadeh M, Sharifpur M, Lingen C. Comparative analysis of five widely-used multi-criteria decision-making methods to evaluate clean energy technologies: A case study. *Sustainability* 2022;14:140314. [\[CrossRef\]](#)
- [3] Uddin MN, Biswas MM, Nuruddin S. Techno-economic impacts of floating PV power generation for remote coastal regions. *Sustain Energy Technol Assess* 2022;51:101930. [\[CrossRef\]](#)
- [4] Qashou Y, Samour A, Abumunshar M. Does the real estate market and renewable energy induce carbon dioxide emissions? Novel evidence from Turkey. *Energies* 2022;15:1-13. [\[CrossRef\]](#)
- [5] Dino IG, Meral Akgül C. Impact of climate change on the existing residential building stock in Turkey: An analysis on energy use, greenhouse gas emissions and occupant comfort. *Renew Energy* 2019;141:828-846. [\[CrossRef\]](#)
- [6] Zhang W, Maleki A. Modeling and optimization of a stand-alone desalination plant powered by solar/wind energies based on back-up systems using a hybrid algorithm. *Energy* 2022;254:124341. [\[CrossRef\]](#)
- [7] Zhou J, Xu Z. Optimal sizing design and integrated cost-benefit assessment of stand-alone microgrid system with different energy storage employing chameleon swarm algorithm: A rural case in Northeast China. *Renew Energy* 2023;202:1110-1137. [\[CrossRef\]](#)
- [8] Yu X, Li W, Maleki A, Rosen MA, Komeili Birjandi A, Tang L. Selection of optimal location and design of a stand-alone photovoltaic scheme using a modified hybrid methodology. *Sustain Energy Technol Assess* 2021;45:101071. [\[CrossRef\]](#)
- [9] Cao Y, Taslimi MS, Dastjerdi SM, Ahmadi P, Ashjaee M. Design, dynamic simulation, and optimal size selection of a hybrid solar/wind and battery-based system for off-grid energy supply. *Renew Energy* 2022;187:1082-1099. [\[CrossRef\]](#)
- [10] Zeljković Č, Mršić P, Erceg B, Lekić Đ, Kitić N, Matić P. Optimal sizing of photovoltaic-wind-diesel-battery power supply for mobile telephony base stations. *Energy* 2022;242:122545. [\[CrossRef\]](#)
- [11] Mahmoudi SM, Maleki A, Rezaei Ochbelagh D. A novel method based on fuzzy logic to evaluate the storage and backup systems in determining the optimal size of a hybrid renewable energy system. *J Energy Storage* 2022;49:104015. [\[CrossRef\]](#)
- [12] Ma Q, Huang X, Wang F, Xu C, Babaei R, Ahmadian H. Optimal sizing and feasibility analysis of grid-isolated renewable hybrid microgrids: Effects of energy management controllers. *Energy* 2022;240:122503. [\[CrossRef\]](#)
- [13] Xu Y, Huang S, Wang Z, Ren Y, Xie Z, Guo J, et al. Optimization based on tabu search algorithm for optimal sizing of hybrid PV/energy storage system: Effects of tabu search parameters. *Sustain Energy Technol Assess* 2022;53:102662. [\[CrossRef\]](#)
- [14] Yi H, Yang X. A metaheuristic algorithm based on simulated annealing for optimal sizing and techno-economic analysis of PV systems with multi-type of battery energy storage. *Sustain Energy Technol Assess* 2022;53:102724. [\[CrossRef\]](#)
- [15] Aziz AS, Tajuddin MFN, Hussain MK, Adzman MR, Ghazali NH, Ramli MAM, Zidane TEK. A new optimization strategy for wind/diesel/battery hybrid energy system. *Energy* 2022;239:122458. [\[CrossRef\]](#)
- [16] Dufo-López R, Champier D, Gibout S, Lujano-Rojas JM, Domínguez-Navarro JA. Optimisation of off-grid hybrid renewable systems with thermoelectric generator. *Energy Convers Manag* 2019;196:1051-1067. [\[CrossRef\]](#)
- [17] Yu J, Ryu JH, Lee IB. A stochastic optimization approach to the design and operation planning of a hybrid renewable energy system. *Appl Energy* 2019;247:212-220. [\[CrossRef\]](#)
- [18] Kang W, Chen M, Lai W, Luo Y. Distributed real-time power management for virtual energy storage systems using dynamic price. *Energy*. 2021;216:119069. [\[CrossRef\]](#)

- [19] Fares D, Fathi M, Mekhilef S. Performance evaluation of metaheuristic techniques for optimal sizing of a stand-alone hybrid PV/wind/battery system. *Appl Energy* 2022;305:117823. [\[CrossRef\]](#)
- [20] Jasim AM, Jasim BH, Baiceanu FC, Neagu BC. Optimized sizing of energy management system for off-grid hybrid solar/wind/battery/biogasifier/diesel microgrid system. *Mathematics* 2023;11:1248. [\[CrossRef\]](#)
- [21] Afolabi T, Farzaneh H. Optimal design and operation of an off-grid hybrid renewable energy system in Nigeria's rural residential area, using fuzzy logic and optimization techniques. *Sustainability* 2023;15:3862. [\[CrossRef\]](#)
- [22] Rangel N, Li H, Aristidou P. An optimisation tool for minimising fuel consumption, costs and emissions from Diesel-PV-Battery hybrid microgrids. *Appl Energy* 2023;335:120748. [\[CrossRef\]](#)
- [23] Pires ALG, Rotella Junior P, Rocha LCS, Peruchi RS, Janda K, Miranda R. Environmental and financial multi-objective optimization: Hybrid wind-photovoltaic generation with battery energy storage systems. *J Energy Storage*. 2023;66:107425. [\[CrossRef\]](#)
- [24] Al Hariri A, Selimli S, Dumrul H. Effectiveness of heat sink fin position on photovoltaic thermal collector cooling supported by paraffin and steel foam: An experimental study. *Appl Therm Eng* 2022;213:118784. [\[CrossRef\]](#)
- [25] Khalili Z, Sheikholeslami M. Investigation of innovative cooling system for photovoltaic solar unit in existence of thermoelectric layer utilizing hybrid nanomaterial and Y-shaped fins. *Sustain Cities Soc* 2023;93:104543. [\[CrossRef\]](#)
- [26] Jasim AM, Jasim BH, Neagu BC, Alhasnawi BN. Efficient optimization algorithm-based demand-side management program for smart grid residential load. *Axioms* 2023;12:33. [\[CrossRef\]](#)
- [27] Akdamar I, Dumrul H, Selimli S, Yilmaz S. Energetic and exergetic analyses of experimentally investigated hybrid solar air heater. *J Energy Eng* 2023;149:1-11. [\[CrossRef\]](#)
- [28] Amuta EO, Orovwode H, Wara ST, Agbetuyi AF, Matthew S, Esisio EF. Materials Today: Proceedings hybrid power microgrid optimization and assessment for an off-grid location in Nigeria. *Mater Today Proc.* 2023. [\[CrossRef\]](#)
- [29] El-Khozondar HJ, El-batta F, El-Khozondar RJ, Nassar Y, Alramlawi M, Alsadi S. Standalone hybrid PV/wind/diesel-electric generator system for a COVID-19 quarantine center. *Environ Prog Sustain Energy* 2022;42. [\[CrossRef\]](#)
- [30] Kelly E, Medjo Nouadje BA, Tonsie Djiela RH, Kapen PT, Tchuen G, Tchinda R. Off grid PV/Diesel/Wind/Batteries energy system options for the electrification of isolated regions of Chad. *Heliyon* 2023;9. [\[CrossRef\]](#)
- [31] Zhang W, Maleki A, Rosen MA. A heuristic-based approach for optimizing a small independent solar and wind hybrid power scheme incorporating load forecasting. *J Clean Prod* 2019;241:117920. [\[CrossRef\]](#)
- [32] Abdelkader A, Rabeh A, Mohamed Ali D, Mohamed J. Multi-objective genetic algorithm based sizing optimization of a stand-alone wind/PV power supply system with enhanced battery/supercapacitor hybrid energy storage. *Energy* 2018;163:351-363. [\[CrossRef\]](#)
- [33] Zhang Z, Wen K, Sun W. Optimization and sustainability analysis of a hybrid diesel-solar-battery energy storage structure for zero energy buildings at various reliability conditions. *Sustain Energy Technol Assess* 2022;55:102913. [\[CrossRef\]](#)
- [34] Güven AF, Samy MM. Performance analysis of autonomous green energy system based on multi and hybrid metaheuristic optimization approaches. *Energy Convers Manag* 2022;269:116058. [\[CrossRef\]](#)
- [35] Yousri D, Farag HEZ, Zeineldin H, El-Saadany EF. Integrated model for optimal energy management and demand response of microgrids considering hybrid hydrogen-battery storage systems. *Energy Convers Manag* 2023;280:116809. [\[CrossRef\]](#)
- [36] Kharrich M, Selim A, Kamel S, Kim J. An effective design of hybrid renewable energy system using an improved Archimedes optimization algorithm: A case study of Farafra, Egypt. *Energy Convers Manag* 2023;283:116907. [\[CrossRef\]](#)
- [37] Nadimi R, Goto M, Tokimatsu K. The impact of diesel operation time constraint on total cost of diesel-based hybrid renewable power system simulation model. *Renew Energy Focus* 2022;44:40-55. [\[CrossRef\]](#)
- [38] Sanni SO, Oricha JY, Oyewole TO, Bawonda FI. Analysis of backup power supply for unreliable grid using hybrid solar PV/diesel/biogas system. *Energy* 2021;227:120506. [\[CrossRef\]](#)
- [39] Merabet A, Al-Durra A, El-Saadany EF. Energy management system for optimal cost and storage utilization of renewable hybrid energy microgrid. *Energy Convers Manag* 2022;252:115116. [\[CrossRef\]](#)
- [40] Mishra S, Saini G, Saha S, Chauhan A, Kumar A, Maity S. A survey on multi-criterion decision parameters, integration layout, storage technologies, sizing methodologies and control strategies for integrated renewable energy system. *Sustain Energy Technol Assess* 2022;52:102246. [\[CrossRef\]](#)
- [41] Yahiaoui A, Tlemçani A. Superior performances strategies of different hybrid renewable energy systems configurations with energy storage units. *Wind Eng* 2022;46:1471-1486. [\[CrossRef\]](#)
- [42] Amupolo A, Nambundunga S, Chowdhury DSP, Grün G. Techno-economic feasibility of off-grid renewable energy electrification schemes: A case study of an informal settlement in Namibia. *Energies* 2022;15:4235. [\[CrossRef\]](#)

- [43] Ahmed EEE, Demirci A, Tercan SM. Optimal sizing and techno-enviro-economic feasibility assessment of solar tracker-based hybrid energy systems for rural electrification in Sudan. *Renew Energy* 2023;205:1057-1070. [\[CrossRef\]](#)
- [44] Maisanam AKS, Biswas A, Sharma KK. Integrated socio-environmental and techno-economic factors for designing and sizing of a sustainable hybrid renewable energy system. *Energy Convers Manag* 2021;247:114709. [\[CrossRef\]](#)
- [45] Hamanah WM, Abido MA, Alhems LM. Optimum sizing of hybrid PV, wind, battery and diesel system using lightning search algorithm. *Arab J Sci Eng* 2020;45:1871-1883. [\[CrossRef\]](#)
- [46] Omotoso HO, Al-Shaalan AM, Farh HMH, Al-Shamma'a AA. Techno-economic evaluation of hybrid energy systems using artificial ecosystem-based optimization with demand side management. *Electronics* 2022;11:204. [\[CrossRef\]](#)
- [47] Talla Konchou FA, Djeudjo Temene H, Tchinda R, Njomo D. Techno-economic and environmental design of an optimal hybrid energy system for a community multimedia centre in Cameroon. *SN Appl Sci* 2021;3:127. [\[CrossRef\]](#)
- [48] Ogunjuyigbe ASO, Ayodele TR, Akinola OA. Optimal allocation and sizing of PV/Wind/Split-diesel/Battery hybrid energy system for minimizing life cycle cost, carbon emission and dump energy of remote residential building. *Appl Energy* 2016;171:153-171. [\[CrossRef\]](#)
- [49] Bajpai P, Dash V. Hybrid renewable energy systems for power generation in stand-alone applications: A review. *Renew Sustain Energy Rev* 2012;16:2926-2939. [\[CrossRef\]](#)
- [50] Singh S, Chauhan P, Singh NJ. Capacity optimization of grid connected solar/fuel cell energy system using hybrid ABC-PSO algorithm. *Int J Hydrogen Energy* 2020;45:10070-10088. [\[CrossRef\]](#)
- [51] Holland JH. Even their creators do not fully understand genetic algorithms. *Sci Am* 1992;267:66-73. [\[CrossRef\]](#)
- [52] Rashedi E, Nezamabadi-pour H, Saryazdi S. GSA: A gravitational search algorithm. *Inf Sci* 2009;179:2232-2248. [\[CrossRef\]](#)
- [53] Wang JS, Song J Di. Function optimization and parameter performance analysis based on gravitation search algorithm. *Algorithms* 2016;9:3. [\[CrossRef\]](#)
- [54] Mirjalili S, Hashim SZM. A new hybrid PSOGSA algorithm for function optimization. *Int Conf Comput Inf Appl Tianjin*: 2010. p. 374-377. [\[CrossRef\]](#)
- [55] Duman S, Yorukeren N, Altas IH. A novel modified hybrid PSOGSA based on fuzzy logic for non-convex economic dispatch problem with valve-point effect. *Int J Electr Power Energy Syst* 2014;64:121-135. [\[CrossRef\]](#)
- [56] Alajmi A, Wright J. Selecting the most efficient genetic algorithm sets in solving unconstrained building optimization problem. *Int J Sustain Built Environ* 2014;3:18-26. [\[CrossRef\]](#)
- [57] Armstrong JS. Combining forecasts. In: Armstrong JS, editor. *Principles of Forecasting*. *Int Ser Oper Res Manag Sci* 2001;30. [\[CrossRef\]](#)
- [58] Pesaran HAM, Nazari-Heris M, Mohammadi-Ivatloo B, Seyedi H. A hybrid genetic particle swarm optimization for distributed generation allocation in power distribution networks. *Energy* 2020;209:118218. [\[CrossRef\]](#)
- [59] Ünler A. Improvement of energy demand forecasts using swarm intelligence: The case of Turkey with projections to 2025. *Energy Policy* 2008;36:1937-1944. [\[CrossRef\]](#)
- [60] Younes M, Benhamida F. Genetic algorithm-particle swarm optimization (GA-PSO) for economic load dispatch. *Przegląd Elektrotechniczny* 2011;369-372.
- [61] Sahoo BM, Pandey HM, Amgoth T. GAPSO-H: A hybrid approach towards optimizing the cluster based routing in wireless sensor network. *Swarm Evol Comput* 2021;60:100772. [\[CrossRef\]](#)